

# GEOTECHNICAL ENGINEERING

# STRENGTH, STRESS-STRAIN AND BULK MODULUS PARAMETERS FOR FINITE ELEMENT ANALYSES OF STRESSES AND MOVEMENTS IN SOIL MASSES

by

J. M. DUNCAN  
PETER BYRNE  
KAI S. WONG  
and  
PHILLIP MABRY

**REPORT NO. UCB/GT/80-01**

AUGUST, 1980

## DEPARTMENT OF CIVIL ENGINEERING



UNIVERSITY OF CALIFORNIA · BERKELEY

*Meavea Holt*

STRENGTH, STRESS-STRAIN AND BULK MODULUS  
PARAMETERS FOR FINITE ELEMENT ANALYSES  
OF STRESSES AND MOVEMENTS IN SOIL MASSES

by

J. M. Duncan

Peter Byrne

Kai S. Wong

and

Phillip Mabry

Report No. UCB/GT/80-01

August, 1980

College of Engineering  
Office of Research Services  
University of California  
Berkeley, California

TABLE OF CONTENTS

	Page No.
<del>INTRODUCTION</del>	
<del>INTRODUCTION</del>	<del>1</del>
<del>HYPERBOLIC STRESS-STRAIN RELATIONSHIPS</del>	
Nonlinear Stress-Strain Curves Represented by Hyperbolas	5
Stress-Dependent Stress-Strain Behavior Represented by Varying $E_i$ and $(\sigma_1 - \sigma_3)_{ult}$ with Confining Pressure	7
Relationship Between $E_t$ and the Stresses	11
Inelastic Behavior Represented By Use of Different Modulus Values for Loading and Unloading	11
Nonlinear Volume Change Accounted for By Using Constant Bulk Modulus	13
Variation of B with Confining Pressure	16
Restrictions on the Range of Values of B	18
Summary of Hyperbolic Parameters	18
<del>TECHNIQUES FOR DETERMINING VALUES OF THE HYPERBOLIC PARAMETERS FROM LABORATORY TEST RESULTS</del>	
Selecting Data and Eliminating Inconsistencies	22
Evaluation of c and $\phi$ for Cohesive Soils	25
Evaluation of $\phi_o$ and $\Delta\phi$ for Cohesionless Soils	30
Evaluation of K and n	32
Evaluation of $K_{ur}$	40
Evaluation of $K_b$ and m	41
Computer Program for Determining Parameter Values	46

	Page No.
<b>COMPILATIONS OF PARAMETER VALUES</b>	50
Parameters for Soils Tested Under Drained Conditions	50
Parameters for Soils Tested Under Undrained Conditions	57
Conservative Parameter Values	58
<b>SUMMARY</b>	65
<b>ACKNOWLEDGMENT</b>	66
<b>REFERENCES</b>	67

**APPENDIX - COMPUTER PROGRAM SP-5** A-1

The following program provides a means of calculating the shear modulus of soil masses with confining pressure, and is independent of the percentage of strength mobilized. At high shear levels this approximation provides a more reasonable means of representing the behavior of a number of soils.

nonlinear finite element analyses of stresses and movements in earth masses. In that report, the parameters employed to represent nonlinear and stress-dependent stress-strain and volume change behavior were:

- (1) Tangent values of Young's modulus ( $E_t$ ) which vary with confining pressure and the percentage of strength mobilized, and
- (2) Tangent values of Poisson's ratio ( $\nu_t$ ) which vary with confining pressure and the percentage of strength mobilized.

Subsequent studies have shown that the volume change behavior of most soils can be modelled with equal accuracy by assuming that the bulk modulus of the soil varies with confining pressure, and is independent of the percentage of strength mobilized. At high stress levels this assumption provides a more reasonable means of representing the mechanical properties of soils.

This report outlines procedures which may be used to determine the required Young's modulus and bulk modulus parameters from conventional laboratory test data. Specifically, the report is concerned with the use of the following parameters to represent the nonlinear and stress-dependent stress-strain and volume change behavior of soils:

- (1) Tangent values of Young's modulus ( $E_t$ ) which vary with confining pressure and the percentage of strength mobilized (exactly the same as in the previous report by Wong and Duncan), and
- (2) Values of bulk modulus ( $B$ ) which vary with confining

pressure and which are independent of the percentage of strength mobilized.

The cyclic soil resistance relationships (32) were developed for use in nonlinear dynamic analysis of soil deformations. In each instance of such analyses the observational behavior of the soil is treated as being linear and the relationship between stress and strain is assumed to be governed by the generalized Hooke's Law of elastic deformation, which may be expressed as follows for conditions of plane strains:

### HYPERBOLIC STRESS-STRAIN RELATIONSHIPS

The hyperbolic stress-strain relationships (22) were developed for use in nonlinear incremental analyses of soil deformations. In each increment of such analyses the stress-strain behavior of the soil is treated as being linear and the relationship between stress and strain is assumed to be governed by the generalized Hooke's Law of elastic deformations, which may be expressed as follows for conditions of plane strain:

$$\begin{Bmatrix} \Delta\sigma_x \\ \Delta\sigma_y \\ \Delta\tau_{xy} \end{Bmatrix} = \frac{3B}{9B - E} \begin{bmatrix} (3B + E) & (3B - E) & 0 \\ (3B - E) & (3B + E) & 0 \\ 0 & 0 & E \end{bmatrix} \begin{Bmatrix} \Delta\varepsilon_x \\ \Delta\varepsilon_y \\ \Delta\gamma_{xy} \end{Bmatrix} \quad (1)$$

in which

$\Delta\sigma_x$  = normal stress increment

$\Delta\sigma_y$  = normal stress increment

$\Delta\tau_{xy}$  = shear stress increment

$\Delta\varepsilon_x$  = normal strain increment

$\Delta\varepsilon_y$  = normal strain increment

$\Delta\gamma_{xy}$  = shear strain increment

E = Young's modulus

B = bulk modulus

By varying the values of Young's modulus and bulk modulus appropriately as the stresses vary within the soil, it is possible using the simple equation (1) to model three important characteristics of the stress-strain behavior of soils, namely, nonlinearity, stress-dependency, and inelasticity. The procedures used to account for these characteristics are described in the following paragraphs.

Nonlinear Stress-Strain Curves Represented by Hyperbolas. Kondner and his co-workers (29, 30), have shown that the stress-strain curves for a number of soils could be approximated reasonably accurate by hyperbolas like the one shown in Fig. 1. This hyperbola can be represented by an equation of the form:

$$(\sigma_1 - \sigma_3) = \frac{\epsilon}{\frac{1}{E_i} + \frac{\epsilon}{(\sigma_1 - \sigma_3)_{ult}}} \quad (2)$$

While other types of curves could also be used, these hyperbolas have two characteristics which make their use convenient:

- (1) The parameters which appear in the hyperbolic equation have physical significance.  $E_i$  is the initial tangent modulus or initial slope of the stress-strain curve and  $(\sigma_1 - \sigma_3)_{ult}$  is the asymptotic value of stress difference which is related closely to the strength of the soil. The value of  $(\sigma_1 - \sigma_3)_{ult}$  is always greater than the compressive strength of the soils, as discussed subsequently.
- (2) The values of  $E_i$  and  $(\sigma_1 - \sigma_3)_{ult}$  for a given stress-strain

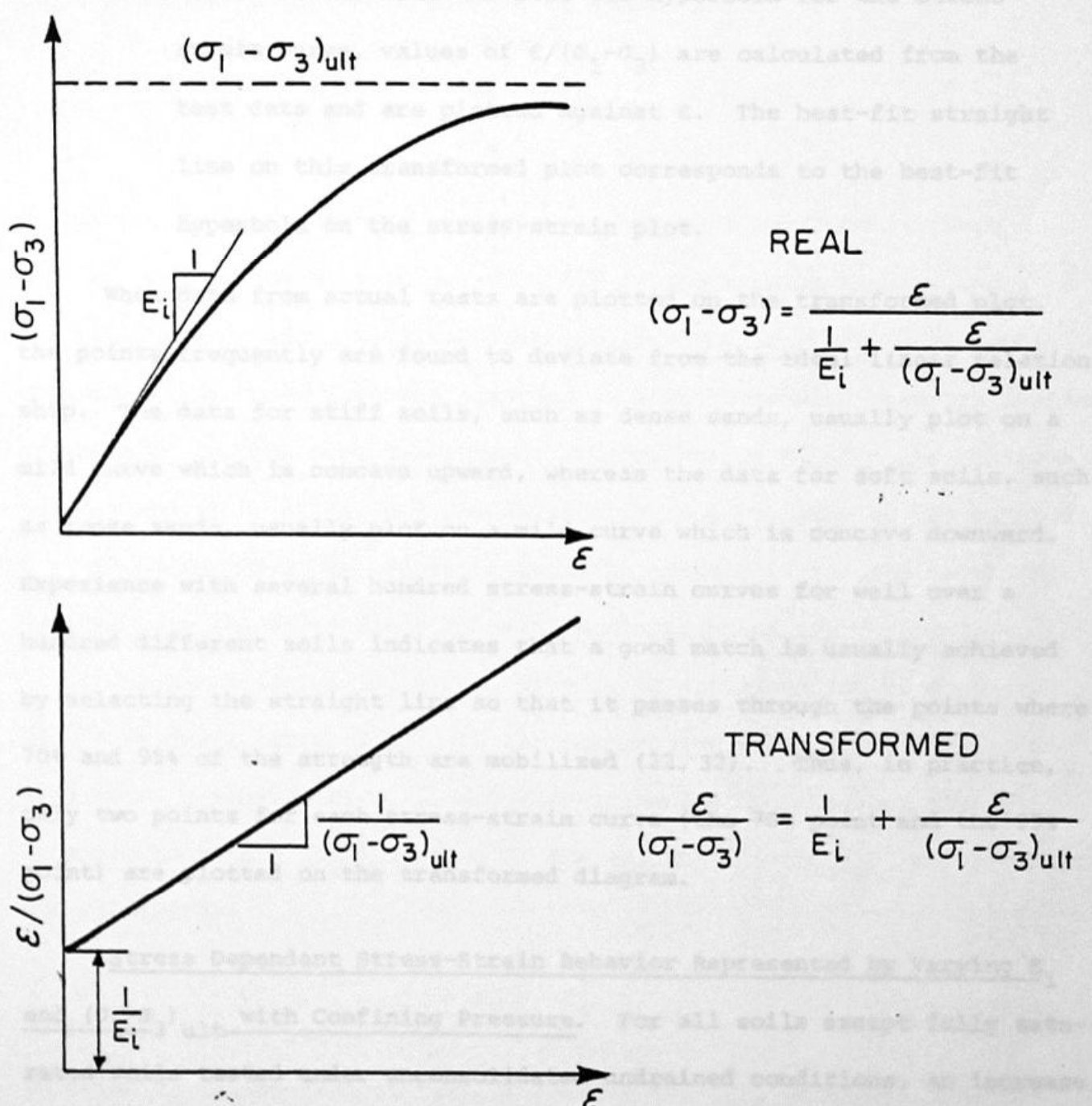


FIG.1 HYPERBOLIC REPRESENTATION OF A STRESS-STRAIN CURVE

curve can be determined easily. If the hyperbolic equation is transformed as shown in the lower part of Fig. 1, it represents a linear relationship between  $\epsilon/(\sigma_1 - \sigma_3)$  and  $\epsilon$ . Thus, to determine the best-fit hyperbola for the stress-strain curve, values of  $\epsilon/(\sigma_1 - \sigma_3)$  are calculated from the test data and are plotted against  $\epsilon$ . The best-fit straight line on this transformed plot corresponds to the best-fit hyperbola on the stress-strain plot.

When data from actual tests are plotted on the transformed plot, the points frequently are found to deviate from the ideal linear relationship. The data for stiff soils, such as dense sands, usually plot on a mild curve which is concave upward, whereas the data for soft soils, such as loose sands, usually plot on a mild curve which is concave downward. Experience with several hundred stress-strain curves for well over a hundred different soils indicates that a good match is usually achieved by selecting the straight line so that it passes through the points where 70% and 95% of the strength are mobilized (22, 32). Thus, in practice, only two points for each stress-strain curve (the 70% point and the 95% point) are plotted on the transformed diagram.

Stress Dependent Stress-Strain Behavior Represented by Varying  $E_i$  and  $(\sigma_1 - \sigma_3)_{ult}$  with Confining Pressure. For all soils except fully saturated soils tested under unconsolidated-undrained conditions, an increase in confining pressure will result in a steeper stress-strain curve and a higher strength, and the values of  $E_i$  and  $(\sigma_1 - \sigma_3)_{ult}$  therefore increase with increasing confining pressure. This stress-dependency is taken into

account by using empirical equations to represent the variations of  $E_i$  and  $(\sigma_1 - \sigma_3)_{ult}$  with confining pressure.

The variation of  $E_i$  with  $\sigma_3$  is represented by an equation of the following form, which was suggested by Janbu (28) :

$$E_i = K p_a \left( \frac{\sigma_3}{p_a} \right)^n \quad (3)$$

The variation of  $E_i$  with  $\sigma_3$  corresponding to this equation is shown in Fig. 2. The parameter  $K$  in equation (3) is the modulus number, and  $n$  is the modulus exponent. Both are dimensionless numbers.  $p_a$  is atmospheric pressure, introduced into the equation to make conversion from one system of units to another more convenient. The values of  $K$  and  $n$  are the same for any system of units, and the units of  $E_i$  are the same as the units of  $p_a$ . To change from one system of units to another it is only necessary to introduce the appropriate value of  $p_a$  in equation (3).

The variation of  $(\sigma_1 - \sigma_3)_{ult}$  with  $\sigma_3$  is accounted for as shown in Fig. 3 by relating  $(\sigma_1 - \sigma_3)_{ult}$  to the compressive strength or stress difference at failure,  $(\sigma_1 - \sigma_3)_f$ , and then using the Mohr-Coulomb strength equation to relate  $(\sigma_1 - \sigma_3)_f$  to  $\sigma_3$ . The values of  $(\sigma_1 - \sigma_3)_{ult}$  and  $(\sigma_1 - \sigma_3)_f$  are related by:

$$(\sigma_1 - \sigma_3)_f = R_f (\sigma_1 - \sigma_3)_{ult} \quad (4)$$

in which  $R_f$  is the failure ratio. Because  $(\sigma_1 - \sigma_3)_f$  is always smaller than  $(\sigma_1 - \sigma_3)_{ult}$ , the value of  $R_f$  is always smaller than unity, and varies from 0.5 to 0.9 for most soils.

The variation of  $(\sigma_1 - \sigma_3)_f$  with  $\sigma_3$  is represented by the familiar Mohr-Coulomb strength relationship, which can be expressed as follows:

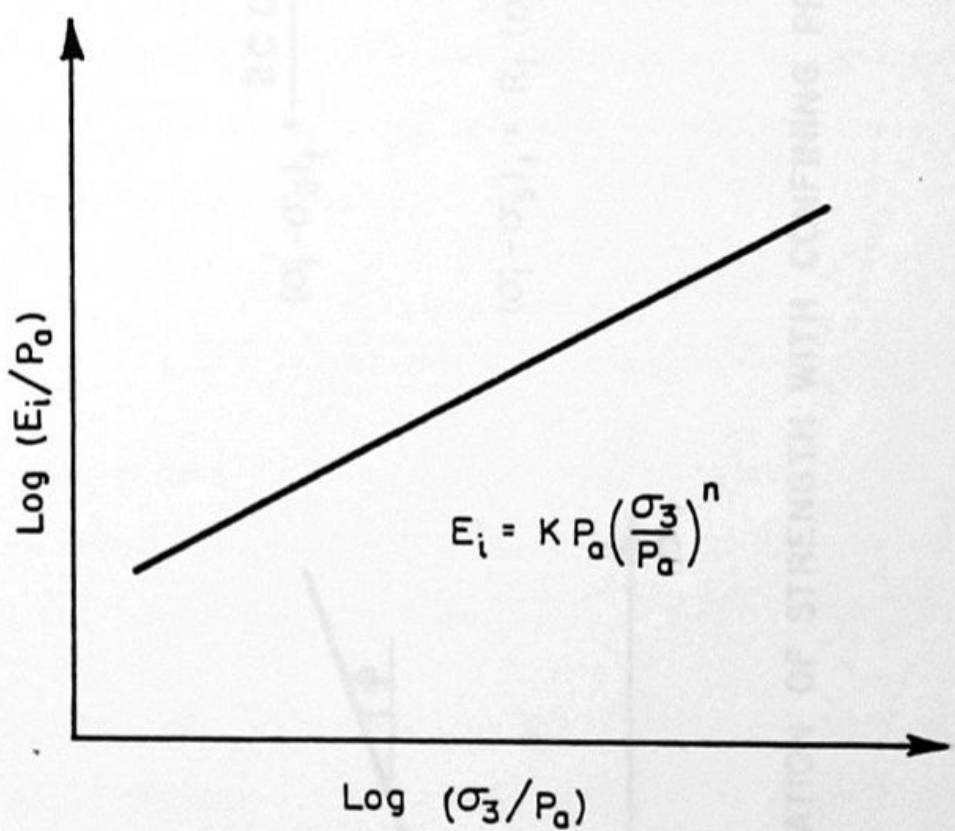


FIG. 2 VARIATION OF INITIAL TANGENT MODULUS  
WITH CONFINING PRESSURE

$$(\sigma_1 - \sigma_3)_f = \frac{2c \cos \phi + 2\sigma_3 \sin \phi}{1 - \sin \phi}$$

$$(\sigma_1 - \sigma_3)_f = R_f (\sigma_1 - \sigma_3)_{ult}$$

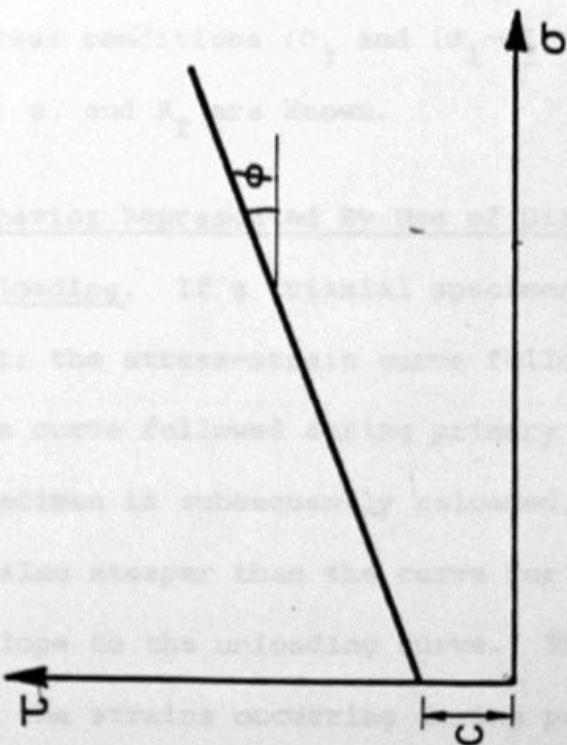


FIG. 3 VARIATION OF STRENGTH WITH CONFINING PRESSURE

$$(\sigma_1 - \sigma_3)_f = \frac{2c \cos\phi + 2\sigma_3 \sin\phi}{1 - \sin\phi} \quad (5)$$

in which  $c$  and  $\phi$  are the cohesion intercept and the friction angle, as shown in Fig. 3.

Relationship Between  $E_t$  and the Stresses. The instantaneous slope of the stress-strain curve is the tangent modulus,  $E_t$ . By differentiating equation (2) with respect to  $\epsilon$  and substituting the expressions of equations (3), (4), and (5) into the resulting expression for  $E_t$ , the following equation can be derived:

$$E_t = \left[ 1 - \frac{R_f(1-\sin\phi)(\sigma_1 - \sigma_3)}{2c \cos\phi + 2\sigma_3 \sin\phi} \right]^2 K_p a \left( \frac{\sigma_3}{p_a} \right)^n \quad (6)$$

This equation can be used to calculate the appropriate value of tangent modulus for any stress conditions ( $\sigma_3$  and  $(\sigma_1 - \sigma_3)$ ) if the values of the parameters  $K$ ,  $n$ ,  $c$ ,  $\phi$ , and  $R_f$  are known.

Inelastic Behavior Represented By Use of Different Modulus Values for Loading and Unloading. If a triaxial specimen is unloaded at some stage during a test, the stress-strain curve followed during unloading is steeper than the curve followed during primary loading, as shown in Fig. 4. If the specimen is subsequently reloaded, the stress-strain curve followed is also steeper than the curve for primary loading and is quite similar in slope to the unloading curve. Thus the soil behavior is inelastic, because the strains occurring during primary loading are only partially recoverable on unloading. On subsequent reloading there is always some hysteresis, but it is usually reasonably accurate to

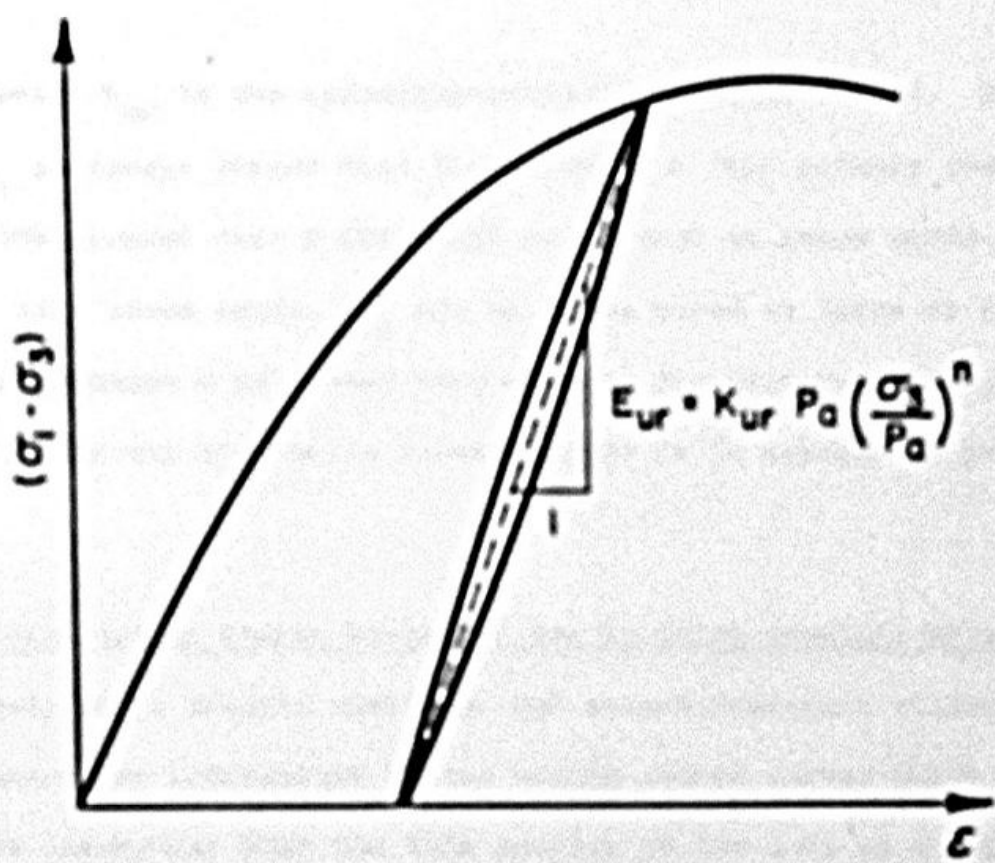


FIG. 4 UNLOADING - RELOADING MODULUS

approximate the behavior during unloading-reloading stress changes as linear and elastic, in effect ignoring any hysteresis effects.

In the hyperbolic stress-strain relationships, the same value of unloading-reloading modulus,  $E_{ur}$ , is used for both unloading and reloading. The value of  $E_{ur}$  is related to the confining pressure by an equation of the same form as equation (3):

$$E_{ur} = K_{ur} p_a \left( \frac{\sigma_3}{p_a} \right)^n \quad (7)$$

In this equation  $K_{ur}$  is the unloading-reloading modulus number. The value of  $K_{ur}$  is always larger than the value of  $K$  (for primary loading).  $K_{ur}$  may be 20% greater than  $K$  for stiff soils such as dense sands. For soft soils, like loose sands,  $K_{ur}$  may be three times as large as  $K$ . The value of the exponent  $n$  is always very similar for primary loading and unloading, and in the hyperbolic relationships it is assumed to be the same.

#### Nonlinear Volume Change Accounted for By Using Constant Bulk

Modulus. Many soils exhibit nonlinear and stress-dependent volume change characteristics, as illustrated by the volume change curves shown in Fig. 5. The assumption that the bulk modulus of the soil is independent of stress level ( $\sigma_1 - \sigma_3$ ) and that it varies with confining pressure provides reasonable approximations to the shapes of these volume change curves. Furthermore, the assumption that the bulk modulus is independent of stress level provides perhaps the best representation of soil behavior which is possible within the framework of incremental elasticity, because it correctly reflects the fact that the response of the soil to changes

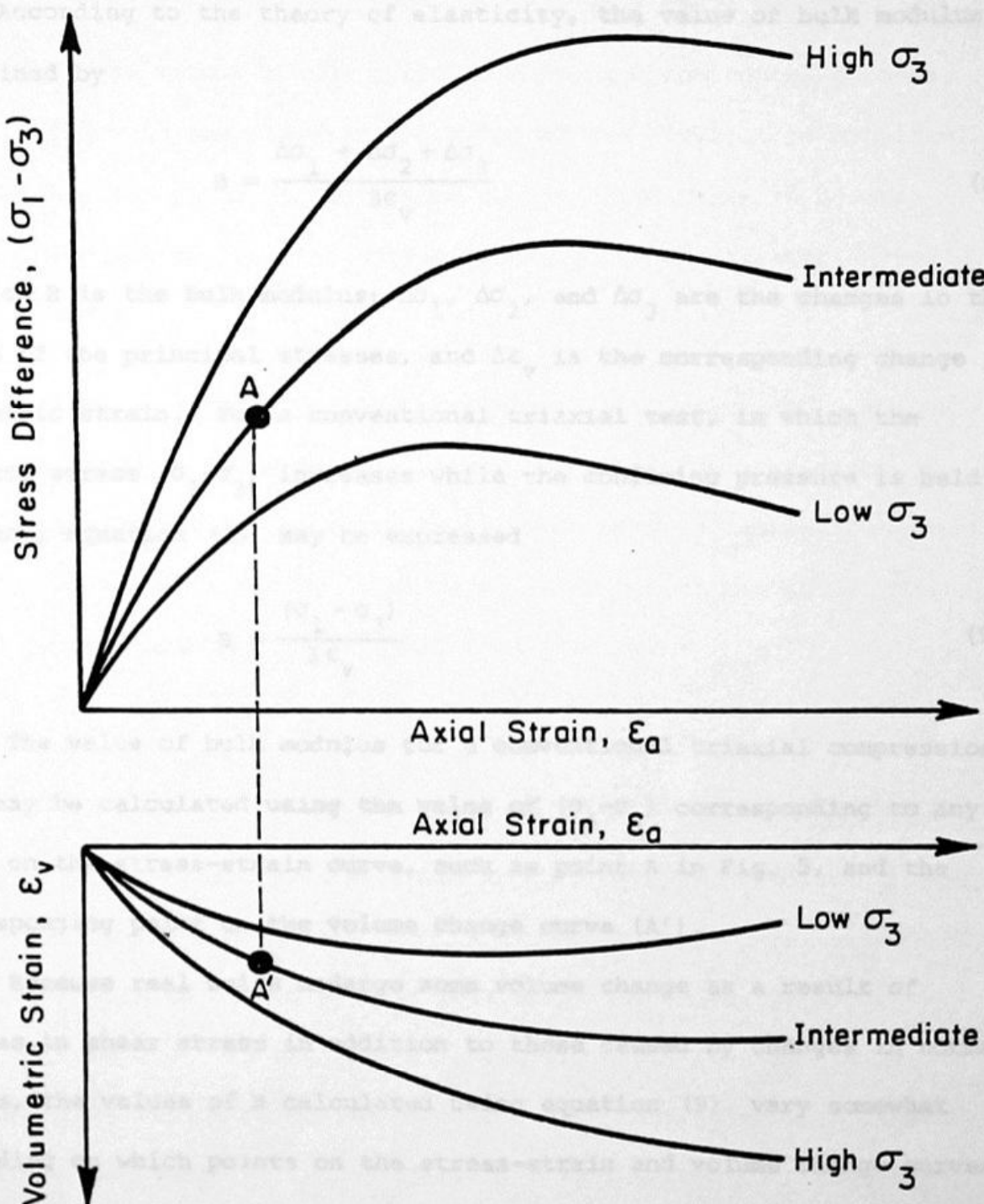


Fig. 5 NONLINEAR AND STRESS-DEPENDENT STRESS-STRAIN AND VOLUME CHANGE CURVES

in mean stress is virtually unaffected by the value of  $(\sigma_1 - \sigma_3)$ .

According to the theory of elasticity, the value of bulk modulus is defined by

$$B = \frac{\Delta\sigma_1 + \Delta\sigma_2 + \Delta\sigma_3}{3\epsilon_v} \quad (8)$$

in which  $B$  is the bulk modulus;  $\Delta\sigma_1$ ,  $\Delta\sigma_2$ , and  $\Delta\sigma_3$  are the changes in the values of the principal stresses, and  $\Delta\epsilon_v$  is the corresponding change in volumetric strain. For a conventional triaxial test, in which the deviator stress  $(\sigma_1 - \sigma_3)$  increases while the confining pressure is held constant, equation (8) may be expressed

$$B = \frac{(\sigma_1 - \sigma_3)}{3\epsilon_v} \quad (9)$$

The value of bulk modulus for a conventional triaxial compression test may be calculated using the value of  $(\sigma_1 - \sigma_3)$  corresponding to any point on the stress-strain curve, such as point A in Fig. 5, and the corresponding point on the volume change curve (A').

Because real soils undergo some volume change as a result of changes in shear stress in addition to those caused by changes in normal stress, the values of  $B$  calculated using equation (9) vary somewhat depending on which points on the stress-strain and volume change curves are employed in the calculation. Study of the volume change behavior of a wide variety of soils has led to the following criteria for selecting which points to use in calculating the value of  $B$ :

- (1) If the volume change curve does not reach a horizontal tangent prior to the stage at which 70% of the strength is

mobilized, use the points on the stress-strain and volume change curves corresponding to a stress level of 70%.

- (2) If the volume change curve does reach a horizontal tangent prior to the stage at which 70% of the strength is mobilized, use the point on the volume change curve where it becomes horizontal, and the corresponding point on the stress-strain curve.

Variation of B with Confining Pressure. When values of B are calculated for tests on the same soil at various confining pressures, the bulk modulus will usually be found to increase with increasing confining pressure. As shown in Fig. 6, the variation of B with confining pressure can be approximated by an equation of the form

$$B = K_b P_a \left( \frac{\sigma_3}{P_a} \right)^m \quad (10)$$

in which  $K_b$  is the bulk modulus number and  $m$  is the bulk modulus exponent, both of which are dimensionless.  $P_a$  is atmospheric pressure, expressed in the same units as  $\sigma_3$  and B. For most soils the values of  $m$  vary between 0.0 and 1.0. In the case of undrained tests on clays compacted dry of optimum, values of  $m$  less than zero have been determined, which corresponds to a decrease in the value of B as the confining pressure increases. This unusual behavior is believed to result from a breakdown in the structural arrangement of the soil particles due to the application of larger pressures.

restrictions on the range of values of  $B$ . As the value of  $B$  approaches zero, the corresponding value of  $V_s$  (tangent Poisson's ratio) approaches zero, because  $V_s = 1/2 - 2/B$ . Therefore in finite element computer programs, the values of  $V_s$  may be restricted to positive values by using  $B = 0/3$  or cause some equation (10) indicates lower values. Similarly, by using  $B = 17\%$ , where equation (10) indicates higher values, the value of  $V_s$  may be restricted to values less than or equal to 0.42.

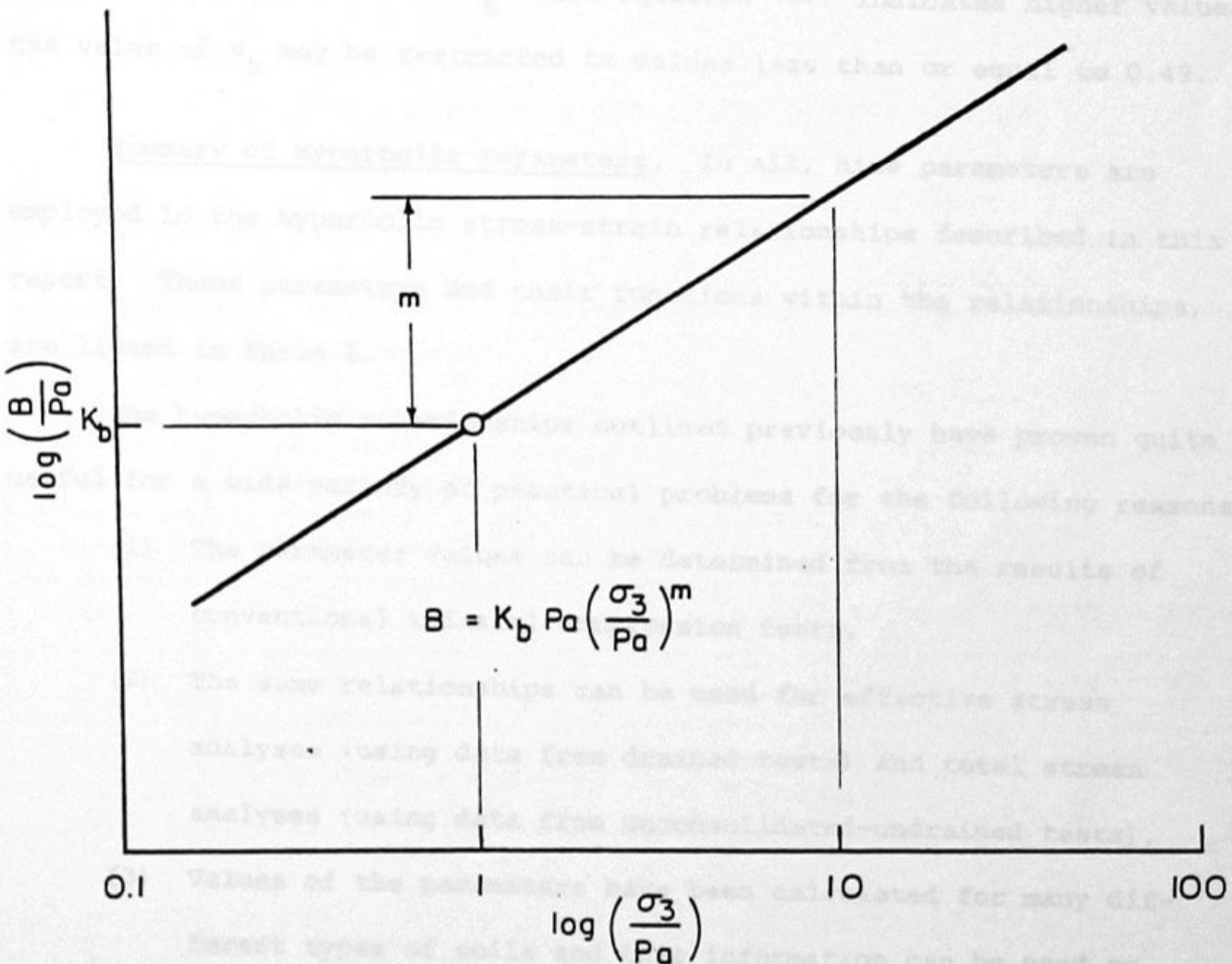


Fig. 6 VARIATION OF BULK MODULUS WITH CONFINING PRESSURE

Restrictions on the Range of Values of B. As the value of B approaches  $E_t/3$ , the corresponding value of  $\nu_t$  (tangent Poisson's ratio) approaches zero, because  $\nu_t = 1/2 - E_t/6B$ . Therefore in finite element computer programs, the values of  $\nu_t$  may be restricted to positive values by using  $B = E_t/3$  in cases where equation (10) indicates lower values. Similarly, by using  $B = 17 E_t$  where equation (10) indicates higher values, the value of  $\nu_t$  may be restricted to values less than or equal to 0.49.

Summary of Hyperbolic Parameters. In all, nine parameters are employed in the hyperbolic stress-strain relationships described in this report. These parameters and their functions within the relationships, are listed in Table 1.

The hyperbolic relationships outlined previously have proven quite useful for a wide variety of practical problems for the following reasons:

- (1) The parameter values can be determined from the results of conventional triaxial compression tests.
- (2) The same relationships can be used for effective stress analyses (using data from drained tests) and total stress analyses (using data from unconsolidated-undrained tests).
- (3) Values of the parameters have been calculated for many different types of soils and this information can be used to estimate reasonable values of the parameters in cases where the available data are insufficient to define the parameters for all of the soils involved in a particular problem. The information is also quite useful for assessing the reliability of parameter values derived from laboratory test results.

The assumptions and relationships have been summarized below which should be understood by anyone who uses them.

- (1) Being based on the generalized Mohr's Law Equation 1, the relationships are most suitable for analysis of stresses and movements prior to failure. The relationships are capable of predicting accurately nonlinear relationships between load and displacement for small strains.

TABLE 1. SUMMARY OF THE HYPERBOLIC PARAMETERS

Parameter	Name	Function
$K, K_{ur}$	Modulus number	
$n$	Modulus exponent	Relate $E_i$ and $E_{ur}$ to $\sigma_3$
$c$	Cohesion intercept	
$\phi, \Delta\phi$	Friction angle parameters	Relate $(\sigma_1 - \sigma_3)_f$ to $\sigma_3$
$R_f$	Failure ratio	Relates $(\sigma_1 - \sigma_3)_{ult}$ to $(\sigma_1 - \sigma_3)_f$
$K_b$	Bulk modulus number	Value of $B/P_a$ at $\sigma_3 = P_a$
$m$	Bulk modulus exponent	Change in $B/P_a$ for ten-fold increase in $\sigma_3$

therefore be limited to soils which exhibit linear elastic behavior and no plastic deformations in response to low confining pressures.

(2) The equations are not fundamental soil mechanics equations but values of empirical coefficients which are determined from tests on the soil under a limited range of conditions. The values of the parameters depend on the history of the test.

The simple hyperbolic relationships have some significant limitations which should be understood by anyone who uses them:

- (1) Being based on the generalized Hooke's Law (equation 1) the relationships are most suitable for analysis of stresses and movements prior to failure. The relationships are capable of predicting accurately nonlinear relationships between loads and movements, and it is possible to continue the analyses up to the stage where there is local failure in some elements. However, when a stage is reached where the behavior of the soil mass is controlled to a large extent by the properties assigned to elements which have already failed, the results will no longer be reliable, and they may be unrealistic in terms of the behavior of real soils at and after failure. These relationships are not useful, therefore, for analyses extending up to the stage of instability of a soil mass. They are useful for predicting movements in stable earth masses.
- (2) The hyperbolic relationships do not include volume changes due to changes in shear stress, or "shear dilatancy." They may therefore be limited in the accuracy with which they can be used to predict deformations in dilatant soils, such as dense sands under low confining pressures.
- (3) The parameters are not fundamental soil properties, but only values of empirical coefficients which represent the behavior of the soil under a limited range of conditions. The values of the parameters depend on the density of the soil, its water

content, the range of pressures used in testing, and the drainage conditions. In order that the parameters will be representative of the behavior of the soil in the field condition, the laboratory test conditions must correspond to the field conditions with regard to these factors.

TECHNIQUES FOR DETERMINING VALUES OF THE HYPERBOLIC  
PARAMETERS FROM LABORATORY TEST RESULTS

The values of the hyperbolic parameters can be determined in a series of simple, straightforward steps using the data from either drained or unconsolidated-undrained triaxial tests. The procedures for evaluating the parameters are described in the following paragraphs.

Selecting Data and Eliminating Inconsistencies. The first step in evaluating the parameters is to select data appropriate to the problem being analyzed. In the case of natural soils, the laboratory tests must be performed using undisturbed specimens. In the case of fill materials, the laboratory tests must be performed using specimens compacted to the same density and water content as in the field. And, in both cases, the drainage conditions in the laboratory tests should correspond to those in the problem being analyzed.

Tests performed at pressures much higher or much lower than those of interest in the problem should not be used in evaluating the parameters, because the values of the parameters which best fit the results of the tests depend to some extent on the range of pressures used in testing.

The test data should be inspected closely to eliminate experimental errors and inconsistencies. For example, in Fig. 7, the stress-strain curve for  $\sigma_3 = 0.95 \text{ kg/cm}^2$  is inconsistent with the data from the remaining four tests, and should be discarded.

Smooth curves should be drawn through the data, using good judgment to make the most reasonable interpretations of all of the test data. For example, in Fig. 8, the data points do not describe smooth variations of

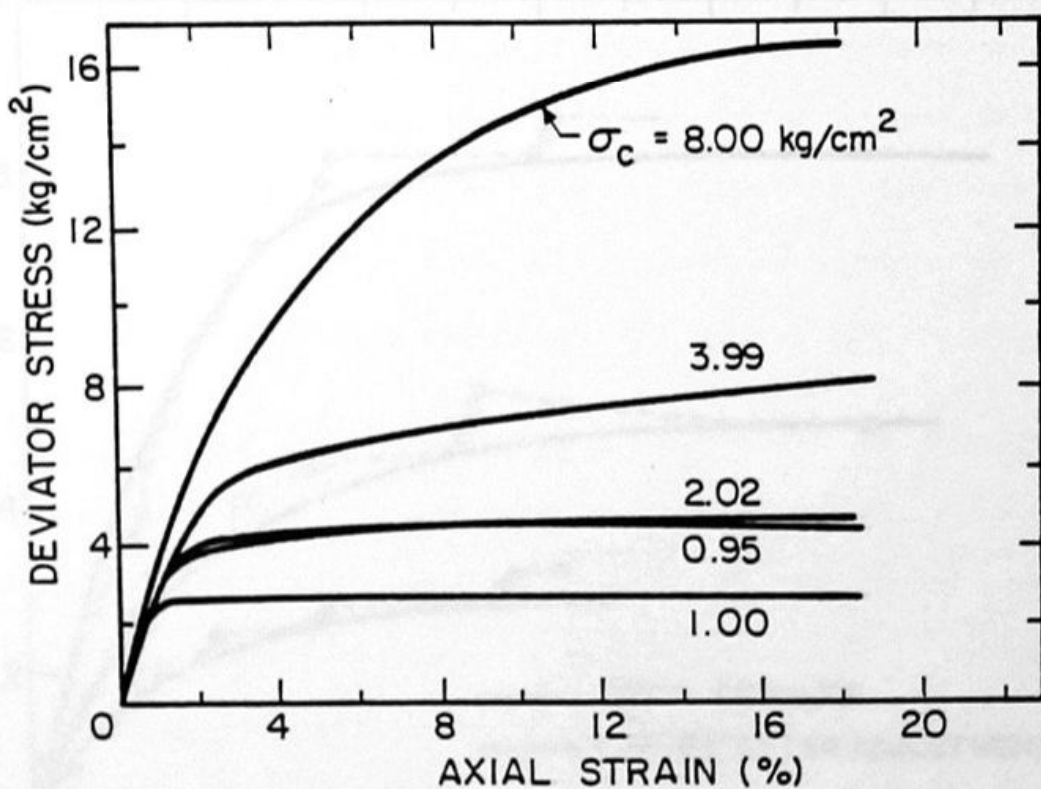


FIG. 7 STRESS-STRAIN CURVES FOR CD TRIAXIAL TESTS, CANYON DAM SILTY CLAY (CL-29C)

shown and should represent differences in the length of time the loads were in place when the initial deformations were measured. The smooth curves represent reasonable interpretations of the data, corresponding to a relatively slow rate of loading.

If necessary, low stress-strain rate volume change curves should be shifted so they pass through the origin. For example, in Fig. 8, the curves A and B shown correspond to the axial strain measured at various times from application of the confining pressures.

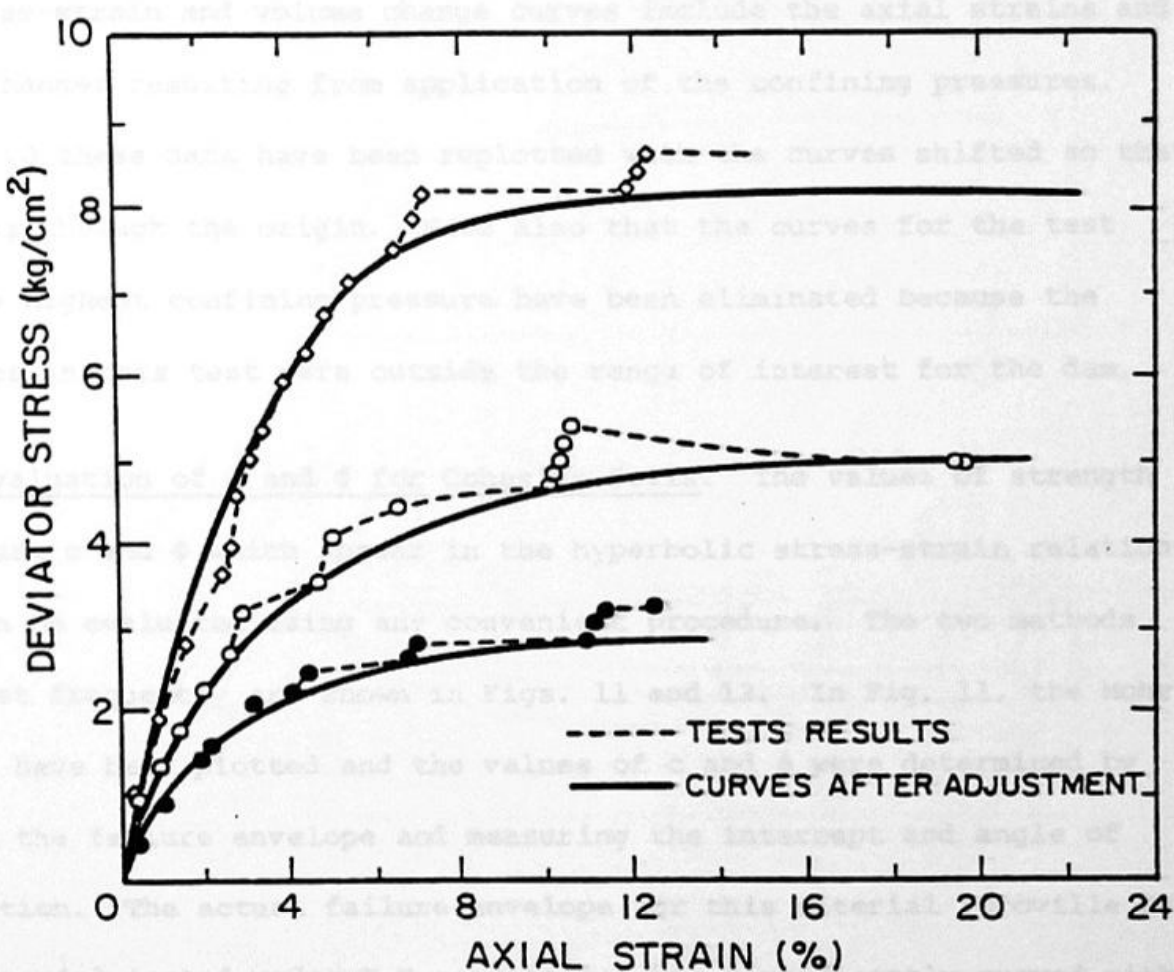


FIG. 8 ADJUSTMENT OF STRESS - STRAIN CURVES

stress and strain because of differences in the length of time the loads were in place when the axial deformations were measured. The smooth curves represent reasonable interpretations of the data, corresponding to a relatively slow rate of loading.

If necessary, the stress-strain and volume change curves should be shifted so that they pass through the origin. For example, in Fig. 9, the stress-strain and volume change curves include the axial strains and volume changes resulting from application of the confining pressures. In Fig. 10 these data have been replotted with the curves shifted so that they pass through the origin. Note also that the curves for the test with the highest confining pressure have been eliminated because the pressures in this test were outside the range of interest for the dam.

Evaluation of c and  $\phi$  for Cohesive Soils. The values of strength parameters  $c$  and  $\phi$  which appear in the hyperbolic stress-strain relationship can be evaluated using any convenient procedure. The two methods used most frequently are shown in Figs. 11 and 12. In Fig. 11, the Mohr's circles have been plotted and the values of  $c$  and  $\phi$  were determined by drawing the failure envelope and measuring the intercept and angle of inclination. The actual failure envelope for this material (Oroville Dam core material tested under U-U conditions) was significantly curved within the range of pressures of interest in the dam, and therefore two sets of strength parameters were used in the analysis of stresses and movements in the dam (31). As shown in Fig. 11, these parameters correspond to two different ranges of pressure.

A second procedure for determining the values of  $c$  and  $\phi$  is illustrated in Fig. 12. This involves plotting the values of  $\frac{1}{2}(\sigma_1 - \sigma_3)$  at

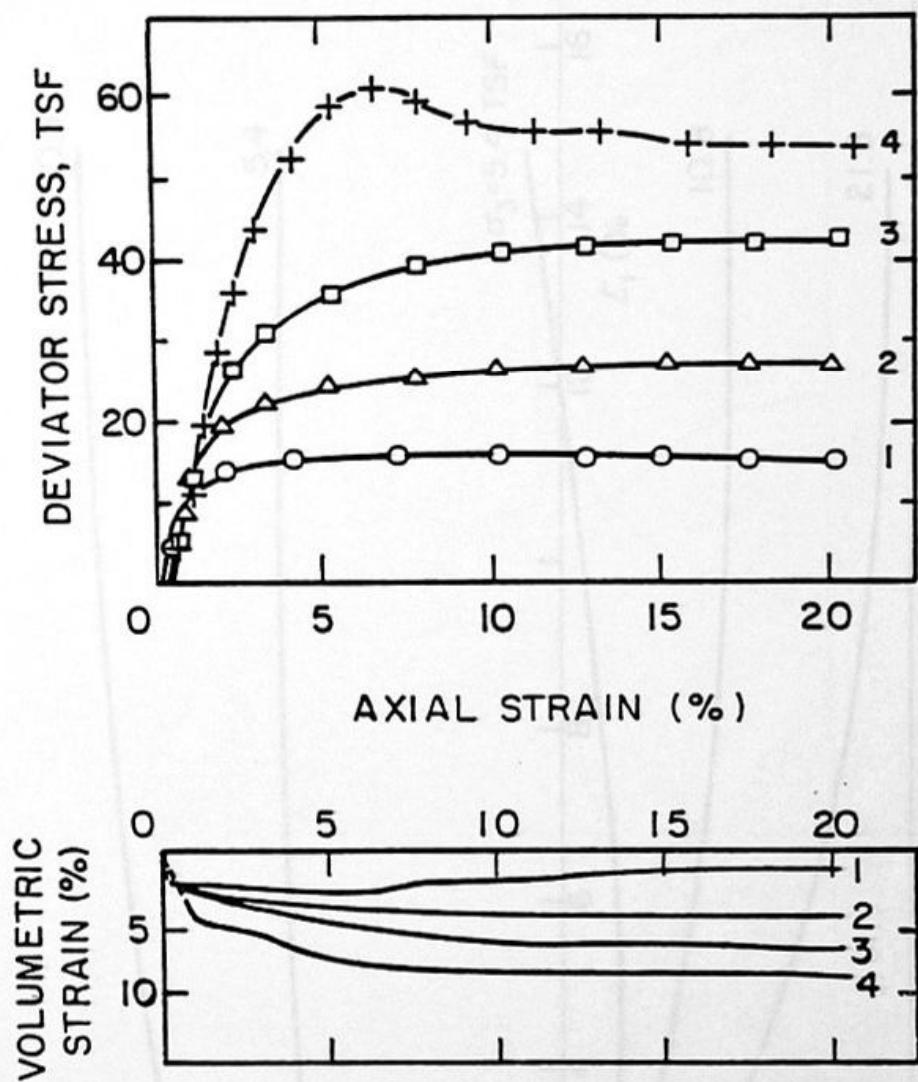


FIG. 9 STRESS-STRAIN AND VOLUME CHANGE CURVES OF UU TRIAXIAL TESTS, NEW DON PEDRO DAM CORE MATERIAL (SC-3)

(BECHTEL, 1969)

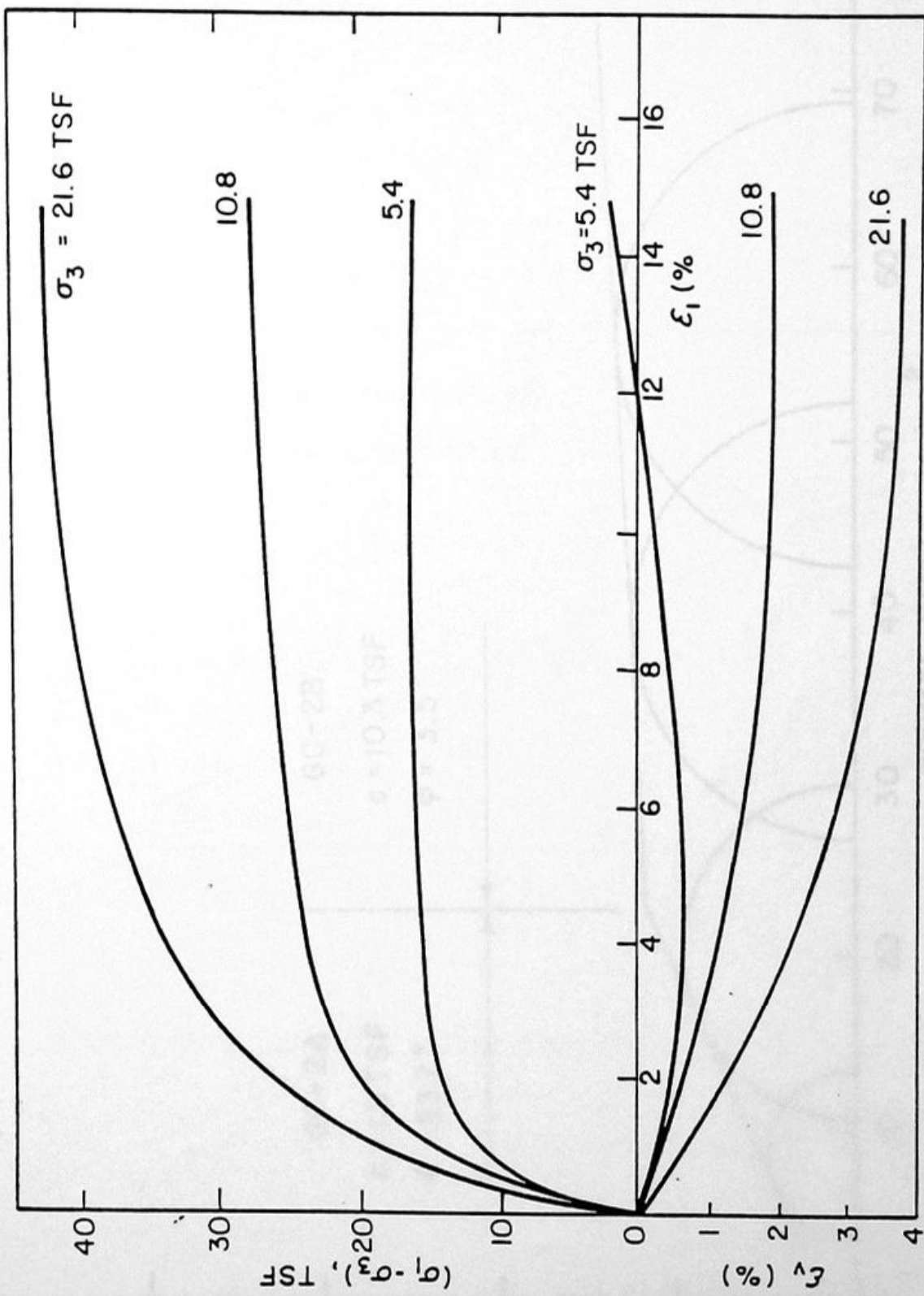
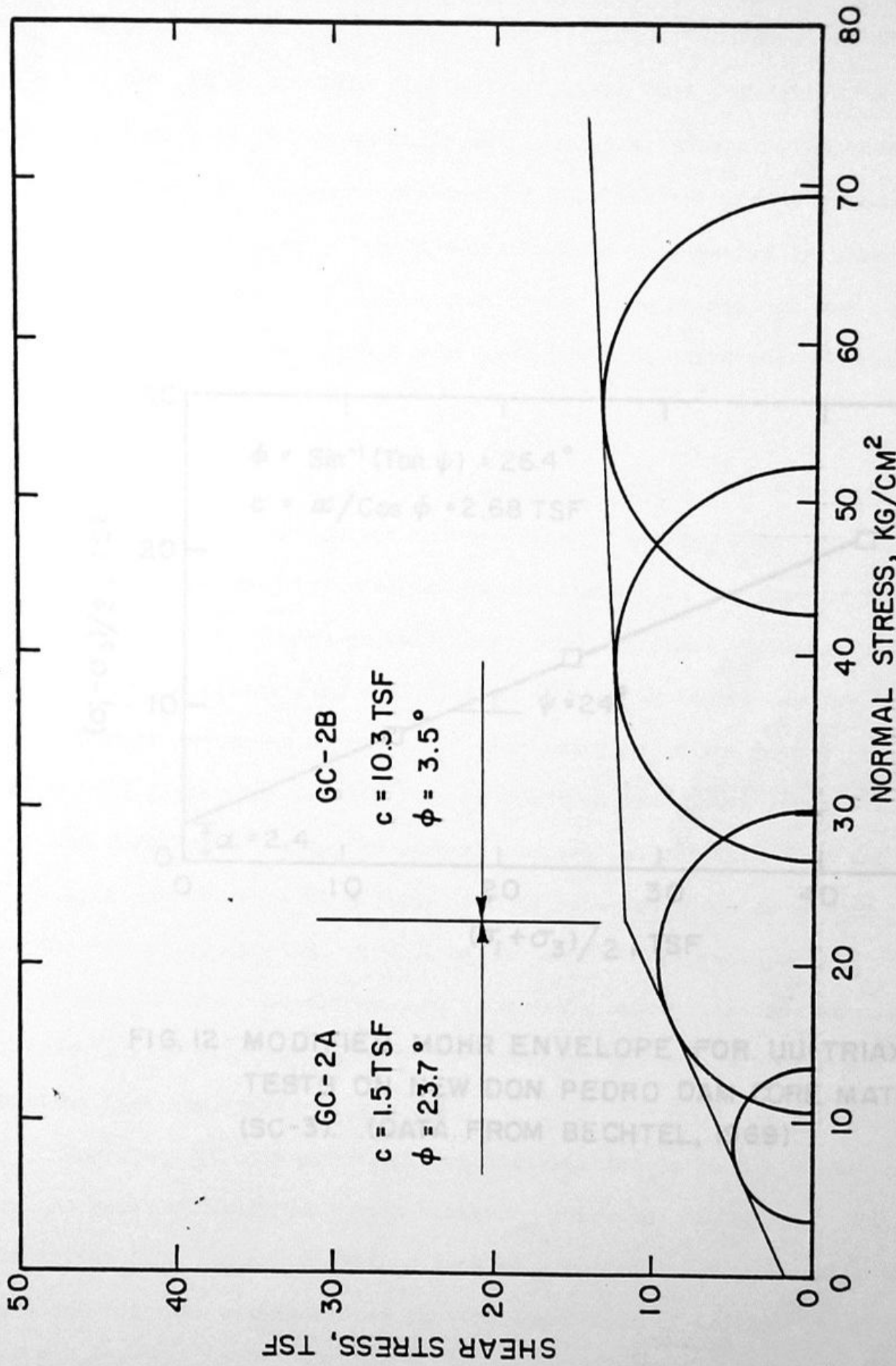


FIG. 10 STRESS-STRAIN AND VOLUME CHANGE CURVES OF NEW DON PEDRO DAM CORE MATERIAL (SC-3), (AFTER ADJUSTMENT)



values against the values of  $(\sigma_1 - \sigma_3)/2$  at failure, the advantage of this method is that it is somewhat simpler to fit the best straight line through a series of points which do not fall in a straight line than it is to draw the best straight envelope for a series of circles which do not have a common tangent. The disadvantage of this method is that the intercept and the angle of inclination of the line in Fig. 12 are not  $c$  and  $\phi$ , and the value of  $c$  and  $\phi$  must be calculated using the equations shown in Fig. 12.

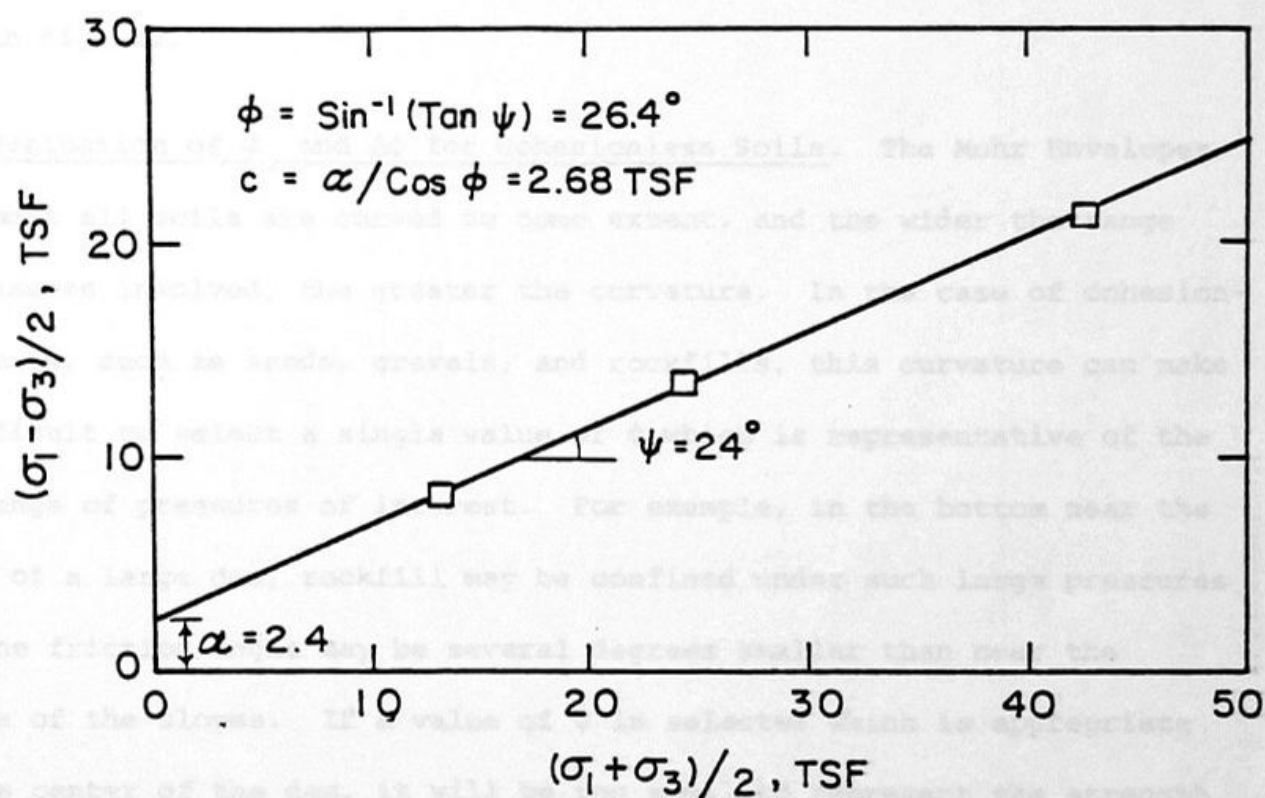


FIG. 12 MODIFIED MOHR ENVELOPE FOR UU-TRIAXIAL TESTS ON NEW DON PEDRO DAM CORE MATERIAL (SC-3). (DATA FROM BECHTEL, 1969)

failure against the values of  $\frac{1}{2}(\sigma_1 + \sigma_3)$  at failure. The advantage of this method is that it is somewhat simpler to fit the best straight line through a series of points which do not fall in a straight line than it is to draw the best straight envelope for a series of circles which do not have a common tangent. The disadvantage of this method is that the intercept and the angle of inclination of the line in Fig. 12 are not  $c$  and  $\phi$ , and the value of  $c$  and  $\phi$  must be calculated using the equations shown in Fig. 12.

Evaluation of  $\phi$  and  $\Delta\phi$  for Cohesionless Soils. The Mohr Envelopes for almost all soils are curved to some extent, and the wider the range of pressures involved, the greater the curvature. In the case of cohesionless soils, such as sands, gravels, and rockfills, this curvature can make it difficult to select a single value of  $\phi$  which is representative of the full range of pressures of interest. For example, in the bottom near the center of a large dam, rockfill may be confined under such large pressures that the friction angle may be several degrees smaller than near the surface of the slopes. If a value of  $\phi$  is selected which is appropriate for the center of the dam, it will be too small to represent the strength of the material near the slopes, and if a value appropriate for the slopes is selected, it will be too large to represent the strength of the material near the center of the dam.

One means of circumventing such difficulties is to use values of  $\phi$  for the material which vary with confining pressure. As shown in Fig. 13, the values of  $\phi$  can be determined from each triaxial test, assuming the envelope for that circle passes through the origin of stress, by using the formula

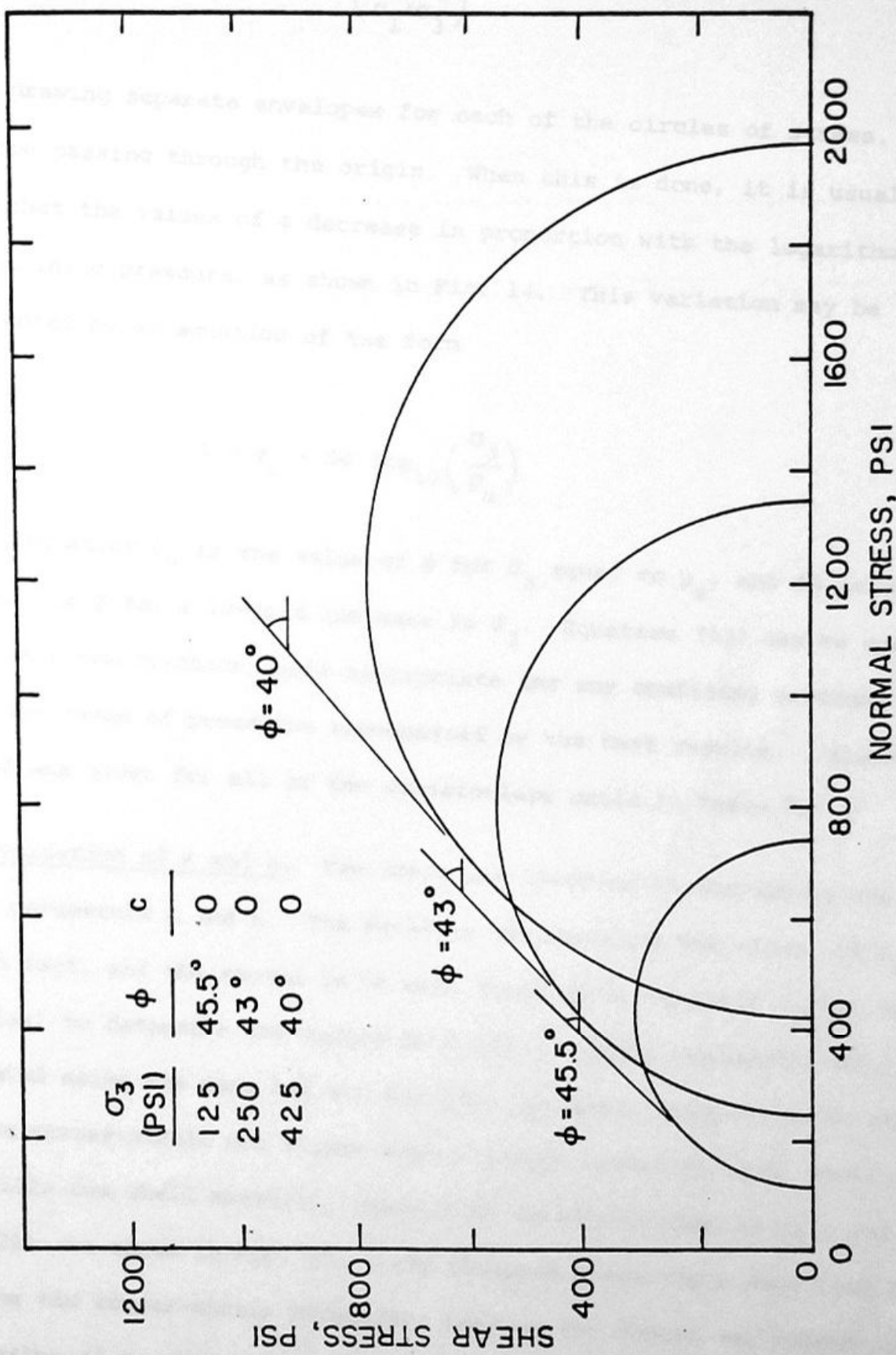


FIG. 13 MOHR ENVELOPE FOR CD-TRIAXIAL TESTS ON OROVILLE DAM SHELL MATERIAL (GP-6). (DATA FROM HALL and GORDON, 1963)

$$\phi = \sin^{-1} \left( \frac{\sigma_1 - \sigma_3}{\sigma_1 + \sigma_3} \right) \quad (11)$$

or by drawing separate envelopes for each of the circles of stress, each envelope passing through the origin. When this is done, it is usually found that the values of  $\phi$  decrease in proportion with the logarithm of the confining pressure, as shown in Fig. 14. This variation may be represented by an equation of the form

$$\phi = \phi_o - \Delta\phi \log_{10} \left( \frac{\sigma_3}{p_a} \right) \quad (12)$$

In this equation  $\phi_o$  is the value of  $\phi$  for  $\sigma_3$  equal to  $p_a$ , and  $\Delta\phi$  is the reduction in  $\phi$  for a 10-fold increase in  $\sigma_3$ . Equation (12) can be used to evaluate the friction angle appropriate for any confining pressure within the range of pressures encompassed by the test results. Values of  $\phi_o$  and  $\Delta\phi$  are given for all of the cohesionless soils in Table 5.

Evaluation of K and n. Two steps are involved in evaluating the modulus parameters K and n. The first is to determine the values of  $E_i$  for each test, and the second is to plot these values against  $\sigma_3$  (on log-log scales) to determine the values of K and n. These procedures will be illustrated using the data for the Oroville Dam shell material as an example.

The stress-strain and volume change-strain curves for four tests on the Oroville Dam shell material, taken from the publication by Hall and Gordon (25) are shown in Fig. 15. Only three of these tests were used in evaluating the stress-strain parameters because the fourth was conducted using a value of  $\sigma_3$  which was beyond the range of interest for the analysis

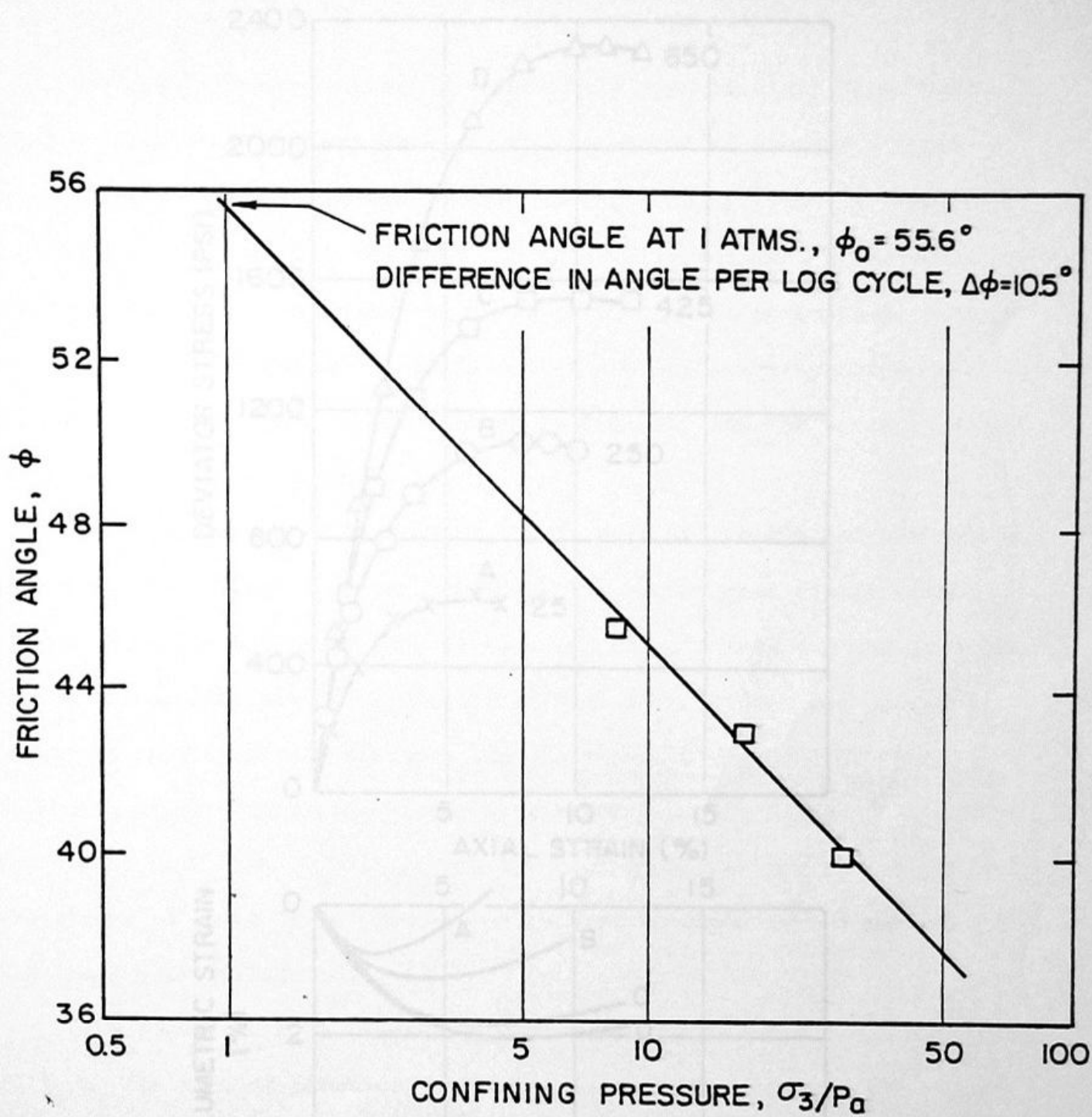


FIG. 14 VARIATION OF FRICTION ANGLE WITH CONFINING PRESSURE FOR OROVILLE DAM SHELL MATERIAL (GP-6).

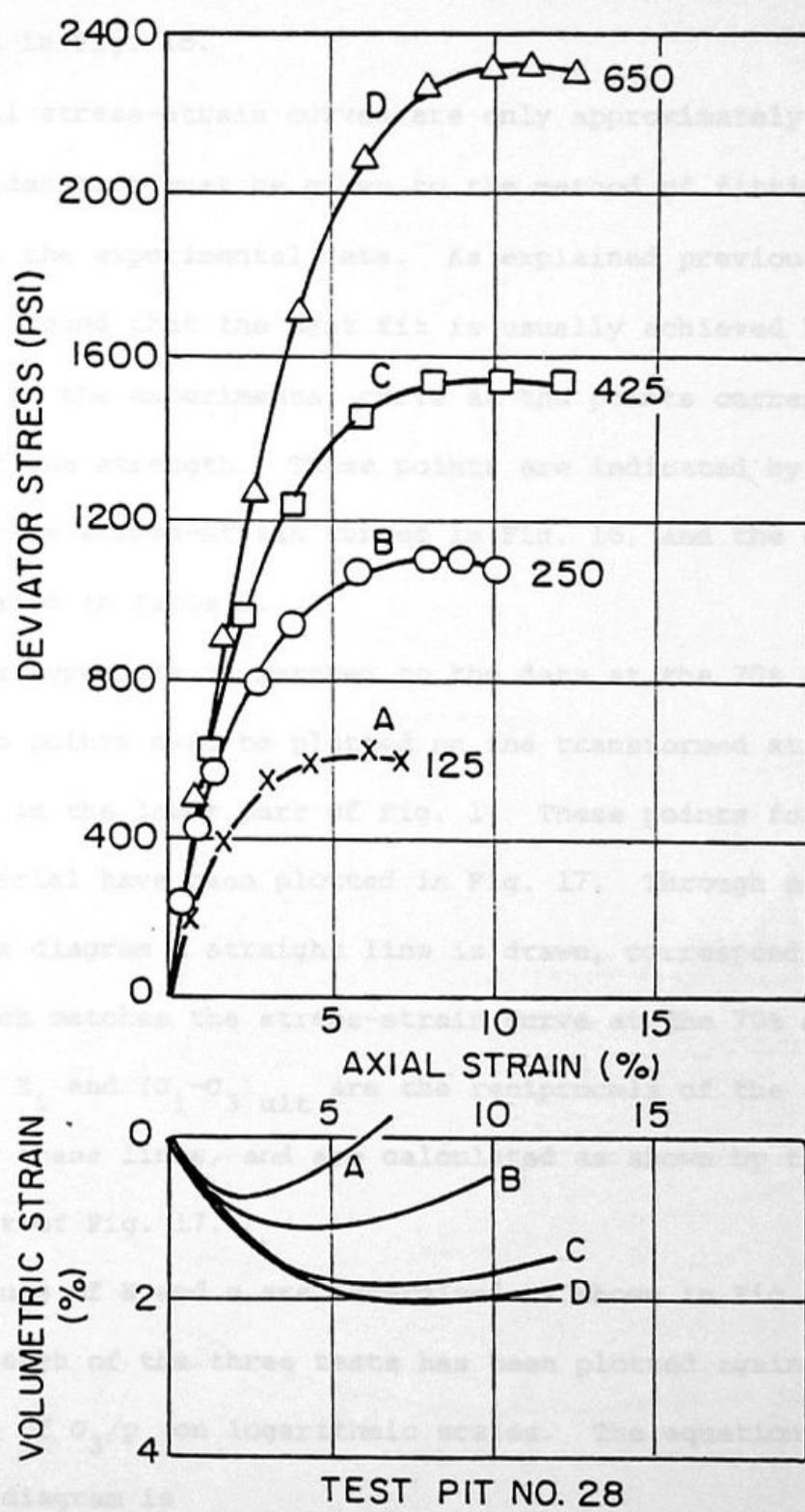


FIG. 15 STRESS-STRAIN AND VOLUME-CHANGE CURVES FROM CD TRIAXIAL TESTS ON OROVILLE DAM SHELL, SILTY SANDY GRAVEL (GP-6). (HALL and GORDON, 1963)

of the dam. The data for the three tests used in the evaluation have been replotted in Fig. 16.

Most real stress-strain curves are only approximately hyperbolic, and some consideration must be given to the method of fitting a hyperbolic curve to the experimental data. As explained previously, Duncan and Chang (22) found that the best fit is usually achieved by matching the hyperbola to the experimental curve at the points corresponding to 70% and 95% of the strength. These points are indicated by arrows for each of the three stress-strain curves in Fig. 16, and the corresponding values are listed in Table 2.

When the hyperbola is matched to the data at the 70% and 95% points, only these two points need be plotted on the transformed stress-strain diagram shown in the lower part of Fig. 1. These points for the Oroville Dam shell material have been plotted in Fig. 17. Through each pair of points on this diagram a straight line is drawn, corresponding to the hyperbola which matches the stress-strain curve at the 70% and 95% points. The values of  $E_i$  and  $(\sigma_1 - \sigma_3)_{ult}$  are the reciprocals of the intercepts and the slopes of these lines, and are calculated as shown by the numbers in the lower part of Fig. 17.

The values of  $K$  and  $n$  are determined as shown in Fig. 18. The value of  $E_i/p_a$  for each of the three tests has been plotted against the corresponding value of  $\sigma_3/p_a$  on logarithmic scales. The equation of a straight line on this diagram is

$$\left(\frac{E_i}{p_a}\right) = K \left(\frac{\sigma_3}{p_a}\right)^n \quad (16)$$

which may be seen to be the same as equation (3). The value of  $K$  is equal

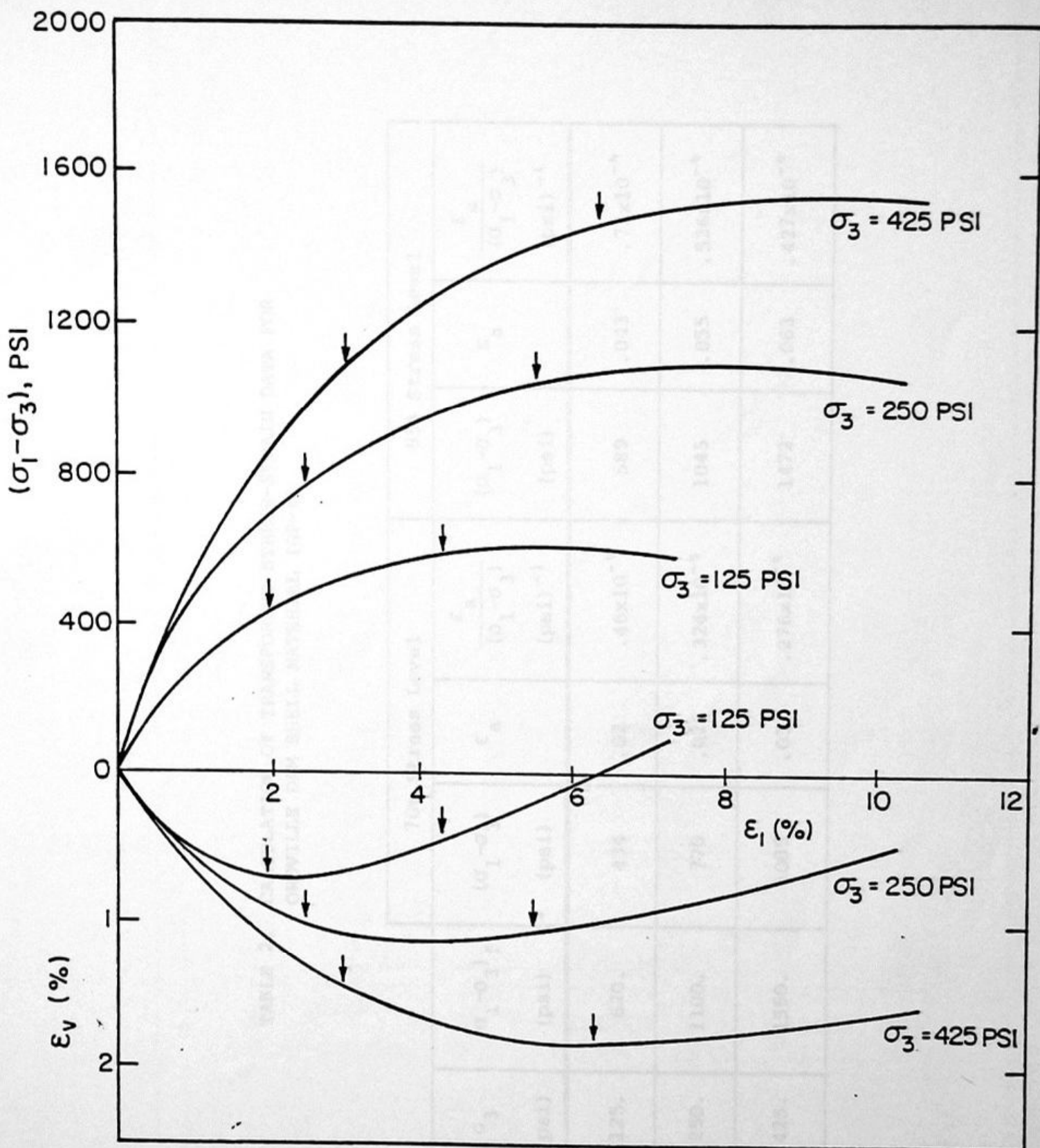


FIG. 16 REPLOTTED STRESS-STRAIN AND VOLUME-CHANGE CURVES FOR OROVILLE DAM SHELL MATERIAL (GP-6).

TABLE 2. CALCULATION OF TRANSFORMED STRESS-STRAIN DATA FOR  
OROVILLE DAM SHELL MATERIAL (GP-6)

$\sigma_3$ (psi)	$(\sigma_1 - \sigma_3)_F$ (psi)	$(\sigma_1 - \sigma_3)$ (psi)	$\epsilon_a$	70% Stress Level		95% Stress Level	
				$\frac{\epsilon_a}{(\sigma_1 - \sigma_3)}$ (psi) <sup>-1</sup>	$(\sigma_1 - \sigma_3)$ (psi)	$\epsilon_a$	$\frac{\epsilon_a}{(\sigma_1 - \sigma_3)}$ (psi) <sup>-1</sup>
125.	620.	434	.02	$.46 \times 10^{-4}$	589	.043	$.73 \times 10^{-4}$
250.	1100.	770	.025	$.324 \times 10^{-4}$	1045	.055	$.526 \times 10^{-4}$
425.	1550.	1085	.03	$.276 \times 10^{-4}$	1472	.063	$.427 \times 10^{-4}$

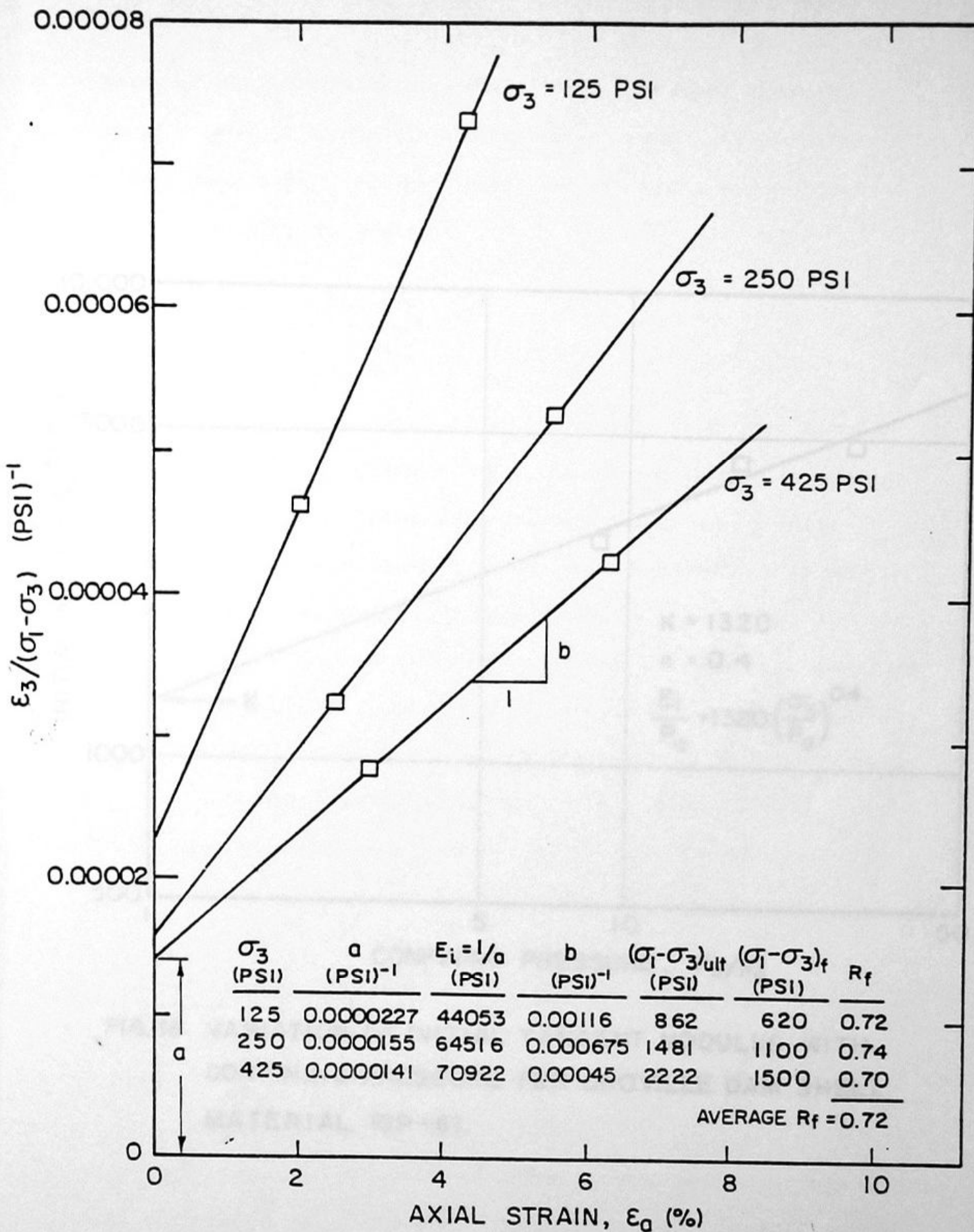


FIG. 17 TRANSFORMED STRESS-STRAIN PLOT FOR OROVILLE DAM SHELL MATERIAL (GP-6).

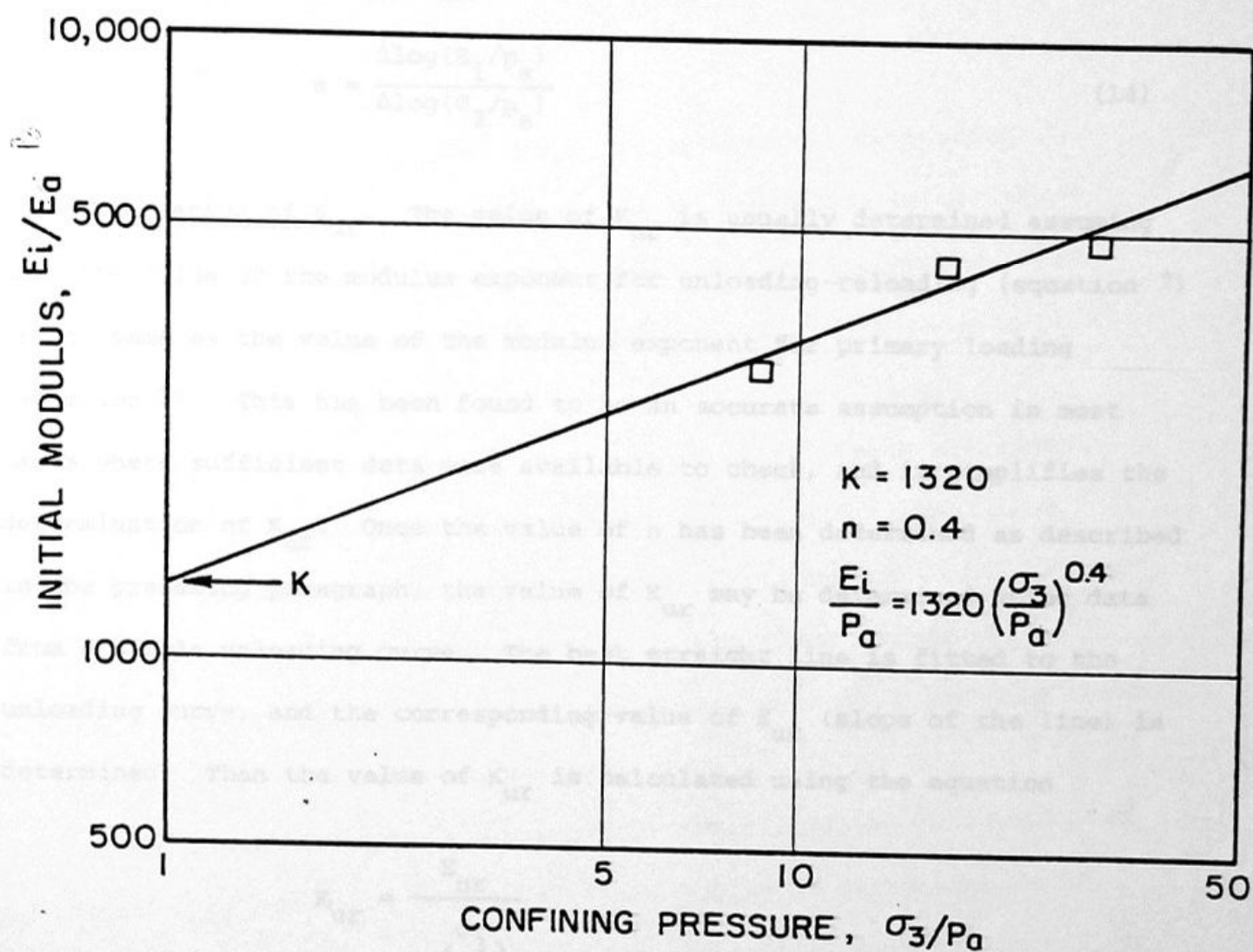


FIG. 18 VARIATION OF INITIAL TANGENT MODULUS WITH CONFINING PRESSURE FOR OROVILLE DAM SHELL MATERIAL (GP-6).

to the value of  $(E_i/p_a)$  at the point where  $(\sigma_3/p_a)$  is equal to unity.

The value of  $n$  is equal to the slope of the line on this plot, and may be determined graphically. Alternatively, the value of  $n$  may be determined numerically using the equation

$$n = \frac{\Delta \log(E_i/p_a)}{\Delta \log(\sigma_3/p_a)} \quad (14)$$

Evaluation of  $K_{ur}$ . The value of  $K_{ur}$  is usually determined assuming that the value of the modulus exponent for unloading-reloading (equation 7) is the same as the value of the modulus exponent for primary loading (equation 3). This has been found to be an accurate assumption in most cases where sufficient data were available to check, and it simplifies the determination of  $K_{ur}$ . Once the value of  $n$  has been determined as described in the preceding paragraph, the value of  $K_{ur}$  may be determined using data from a single unloading curve. The best straight line is fitted to the unloading curve, and the corresponding value of  $E_{ur}$  (slope of the line) is determined. Then the value of  $K_{ur}$  is calculated using the equation

$$K_{ur} = \frac{E_{ur}}{\sigma_3^n p_a \left( \frac{\sigma_3}{p_a} \right)}$$

In this equation  $\sigma_3$  is the value of confining pressure during unloading, and  $n$  is the modulus exponent for primary loading.

Frequently, data for unloading is not available, and it is necessary to assume the value of  $K_{ur}$ . The available data indicate that the value of  $K_{ur}$  is always greater than the value of  $K$ . The ratio  $K_{ur}/K$  varies from

about 1.2 for stiff soils such as dense sands up to 3 or so for softer soils such as loose sands. If the zones undergoing unloading and/or reloading are not large and do not have a dominant effect on the results of the analysis, assuming the value of  $K_{ur}$  within the range from 1.2K to 3K is probably sufficiently accurate.

Evaluation of  $K_b$  and  $m$ . Two steps are involved in determining the values of the bulk modulus parameters  $K_b$  and  $m$ . The first is to determine the value of  $B$  using the data from each test, and the second is to plot these values of  $B$  against  $\sigma_3$  on log-log scales to determine the values of  $K_b$  and  $m$ .

For soils with volume change curves which do not reach horizontal tangents prior to the stage at which 70% of the strength is mobilized, the values of  $B$  are calculated using equation (9) together with  $(\sigma_1 - \sigma_3) = 0.7 (\sigma_1 - \sigma_3)_f$ , and the corresponding value of  $\epsilon_v$ . These points are indicated on the stress-strain and volume change curves for the Mica Creek Dam core material, which are shown in Fig. 19.

For purposes of organizing the calculations involved in determining the values of  $K_b$  and  $m$ , as well as  $K$ ,  $n$  and  $R_f$ , it is convenient to use the calculation form which is shown in Fig. 20. An example of the use of this form for the Mica Dam Core Material is shown in Fig. 21. The hyperbolic stress-strain curves are shown with the test data in Fig. 22.

For highly dilatant soils having volumetric strain curves which reach horizontal tangents prior to the stage of the test at which 70% of the strength is mobilized, the data corresponding to the stage at which the volumetric strain curves become horizontal are used in calculating values of  $B$ . The volume change curves for Monterey No. 0 sand which are

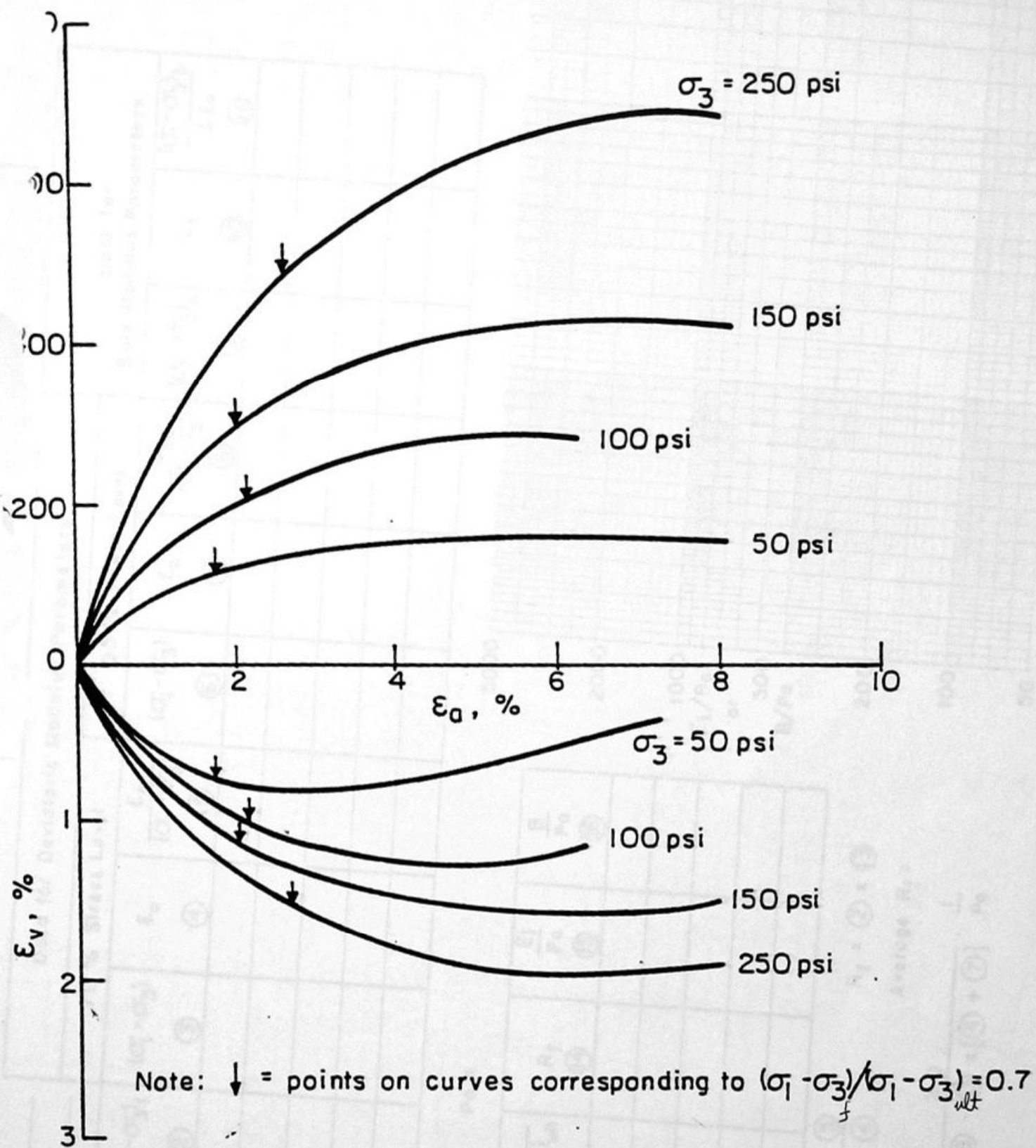


Fig. 19 STRESS-STRAIN AND VOLUME CHANGE CURVES FOR  
MICA CREEK DAM CORE MATERIAL (SM-SC-IB)  
(INSLEY AND HILLIS, 1965)

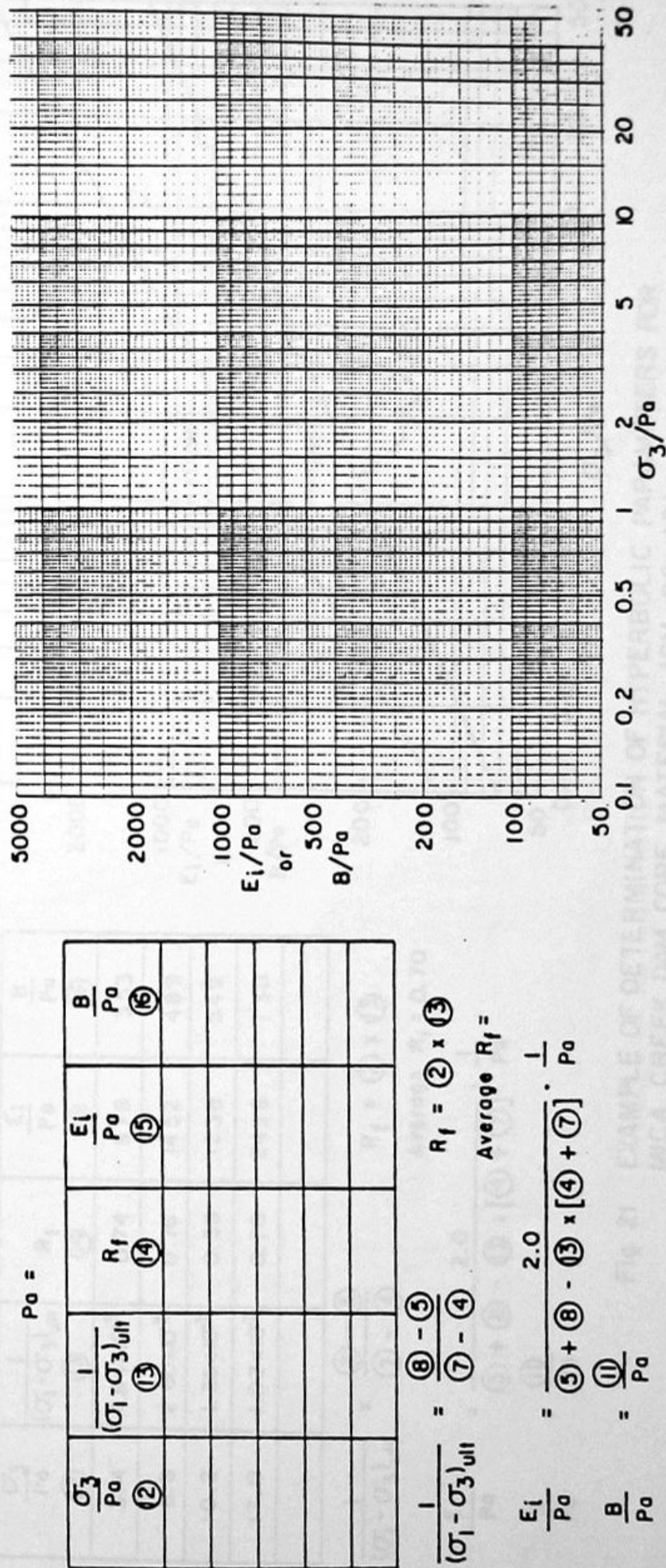


Fig. 20 FORM FOR COMPUTING HYPERBOLIC PARAMETERS

Soil: Mica-Creek  
Data for Deviatoric Modulus Parameters

Core Material	70 % Stress Level						95 % Stress Level			Data for Bulk Modulus Parameters		
	$\sigma_3^1$ (psi) (①)	$(\sigma_1 - \sigma_3)_1$ (psi) (②)	$(\sigma_1 - \sigma_3)_1$ (psi) (③)	$\epsilon_0$ (%) (④)	$(\sigma_1 - \sigma_3)_1$ (psi) (⑤)	$\epsilon_0$ (%) (⑥)	$(\sigma_1 - \sigma_3)_1$ (psi) (⑦)	$\epsilon_0$ (%) (⑧)	$(\sigma_1 - \sigma_3)_1$ (psi) (⑨)	$\epsilon_v$ (%) (⑩)	$\frac{(\sigma_1 - \sigma_3)_b}{3\epsilon_v}$ (⑪)	
50	160	112	0.0180	1.61x10 <sup>-4</sup>	152	0.040	2.63x10 <sup>-4</sup>	112	0.72	5185		
100	293	205	0.0208	1.01x10 <sup>-4</sup>	278	0.047	1.69x10 <sup>-4</sup>	205	0.95	7193		
150	426	298	0.0275	9.23x10 <sup>-5</sup>	405	0.050	1.23x10 <sup>-4</sup>	298	1.23	8076		
250	690	483	0.0260	5.38x10 <sup>-5</sup>	656	0.054	8.23x10 <sup>-5</sup>	483	1.50	10,733		

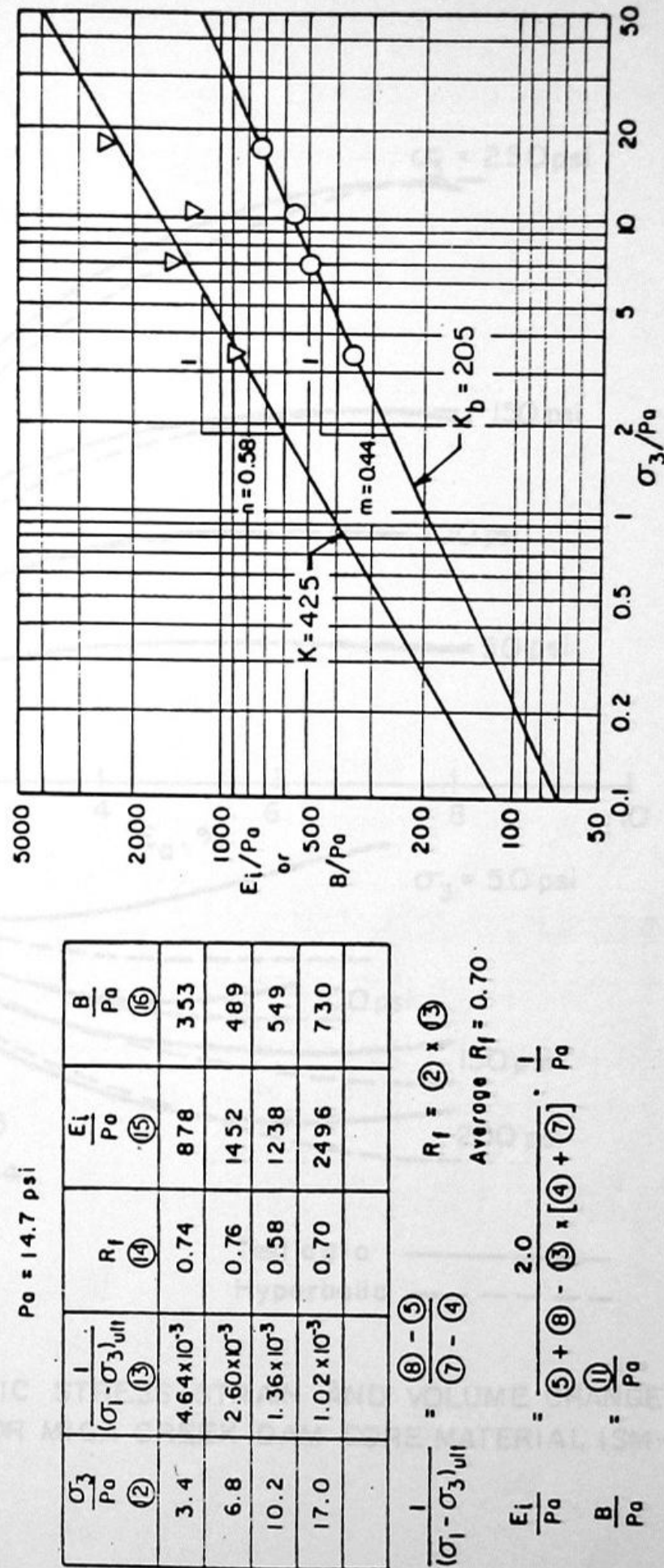


Fig. 21 EXAMPLE OF DETERMINATION OF HYPERBOLIC PARAMETERS FOR MICA CREEK DAM CORE MATERIAL (SM-SC-IB)

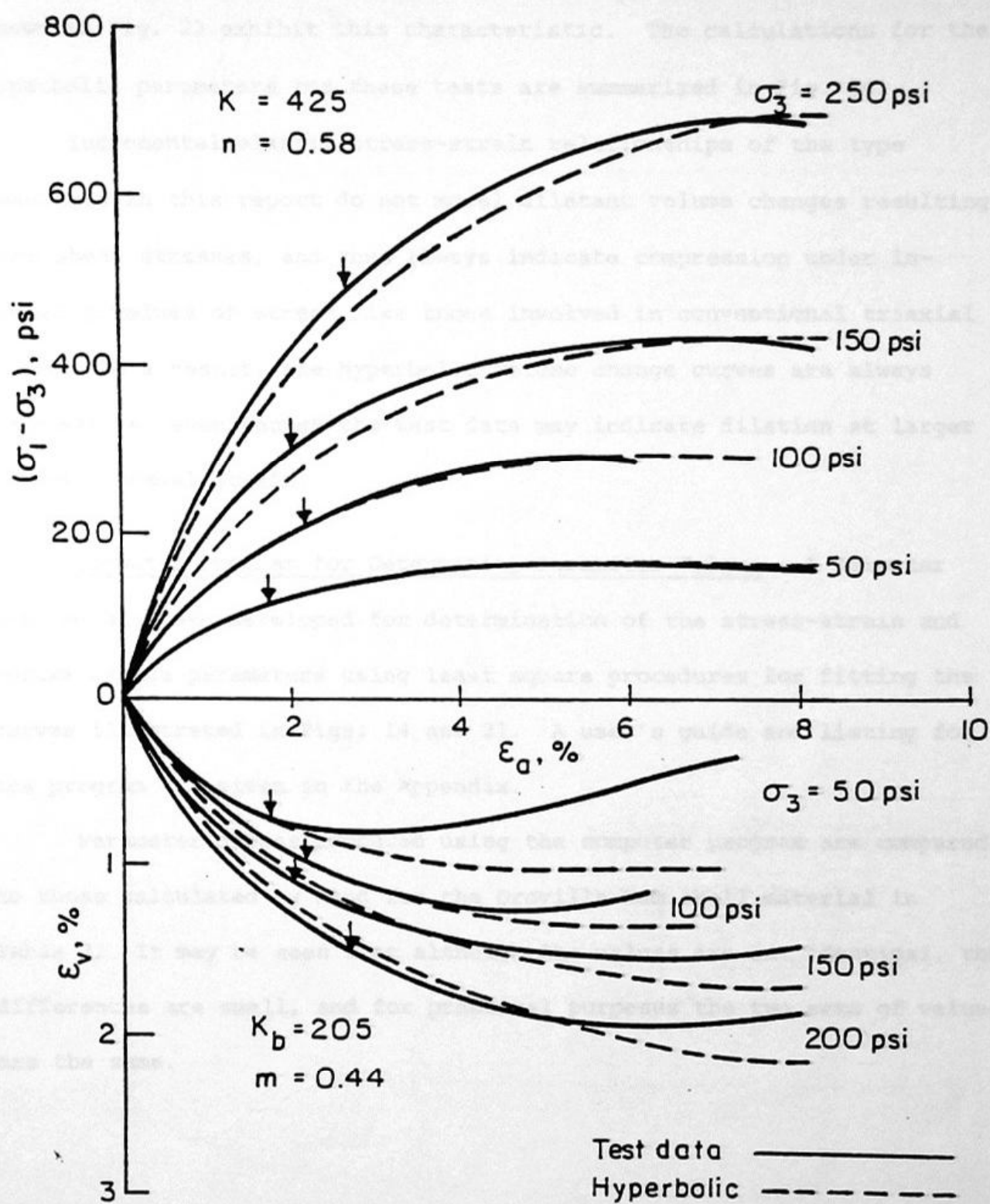


Fig. 22 HYPERBOLIC STRESS-STRAIN AND VOLUME CHANGE CURVES FOR MICA CREEK DAM CORE MATERIAL (SM-SC-IB)

shown in Fig. 23 exhibit this characteristic. The calculations for the hyperbolic parameters for these tests are summarized in Fig. 24.

Incremental elastic stress-strain relationships of the type described in this report do not model dilatant volume changes resulting from shear stresses, and thus always indicate compression under increasing values of stress like those involved in conventional triaxial tests. As a result, the hyperbolic volume change curves are always compressive, even though the test data may indicate dilation at larger values of axial strain.

Computer Program for Determining Parameter Values. A computer program has been developed for determination of the stress-strain and volume change parameters using least square procedures for fitting the curves illustrated in Figs. 14 and 21. A user's guide and listing for the program are given in the Appendix.

Parameter values computed using the computer program are compared to those calculated by hand for the Oroville Dam shell material in Table 3. It may be seen that although the values are not identical, the differences are small, and for practical purposes the two sets of values are the same.

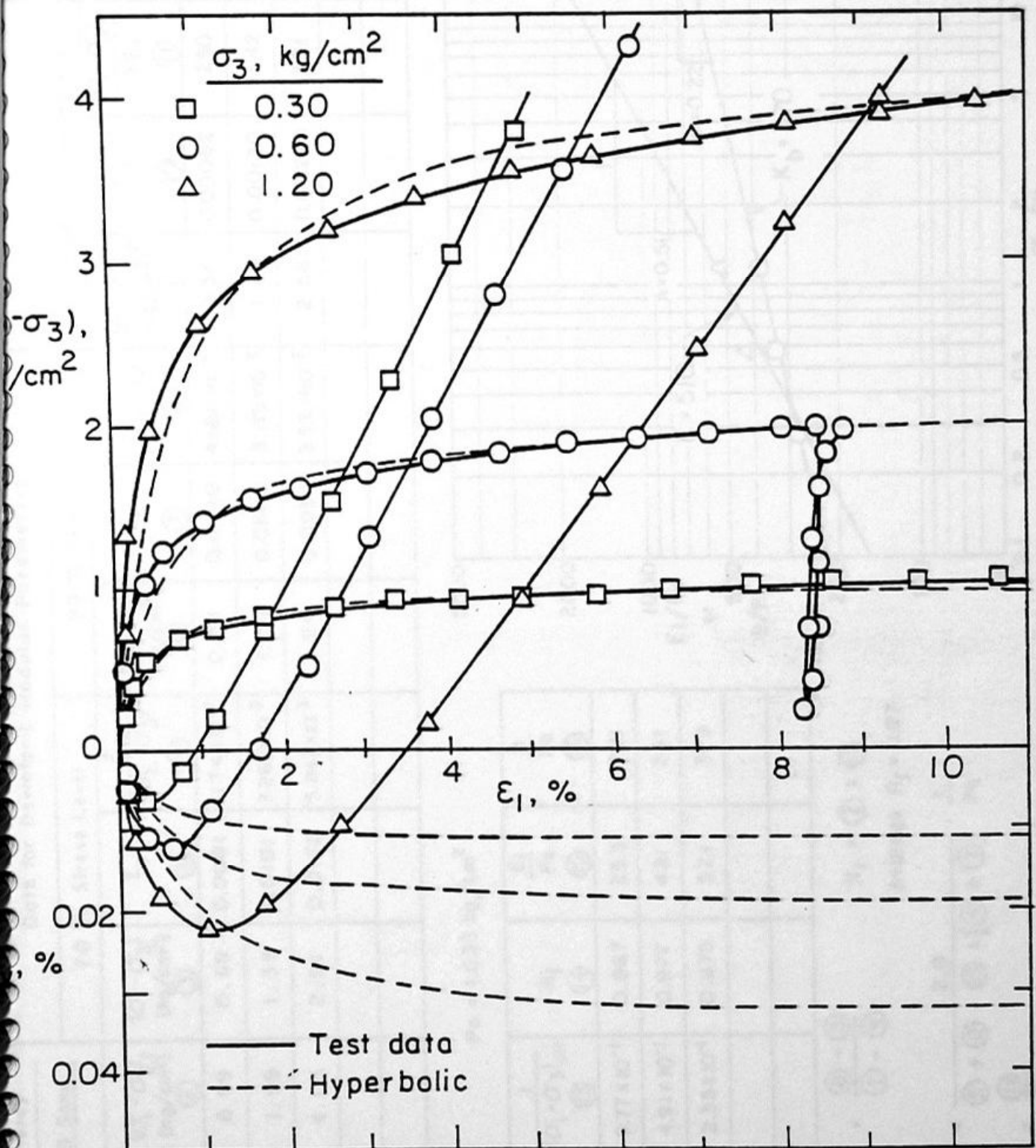


Fig. 23 HYPERBOLIC STRESS-STRAIN AND VOLUME CHANGE CURVES FOR MONTEREY NO. 0 SAND (SP-17 B)  
(LADE, 1971)

No. O Sand	70 % Stress Level						95 % Stress Level					
	$\sigma_3$ (kg/cm <sup>2</sup> )	$(\sigma_1 - \sigma_3)$ (kg/cm <sup>2</sup> )	$\epsilon_a$	$\frac{\epsilon_a}{(\sigma_1 - \sigma_3)}$	$(\sigma_1 - \sigma_3)$ (kg/cm <sup>2</sup> )	$\epsilon_a$	$\frac{\epsilon_a}{(\sigma_1 - \sigma_3)}$	$\frac{\epsilon_a}{(\sigma_1 - \sigma_3)}$ (kg/cm <sup>2</sup> )	$\epsilon_v$	$\frac{(\sigma_1 - \sigma_3)_b}{3 \epsilon_v}$	$\frac{(\sigma_1 - \sigma_3)_b}{3 \epsilon_v}$	
0.30	0.99	0.69	0.0081	1.174 x 10 <sup>-2</sup>	0.94	0.0440	4.681 x 10 <sup>-2</sup>	0.54	0.00062	290		
0.60	1.99	1.39	0.0101	7.266 x 10 <sup>-3</sup>	1.89	0.0600	3.175 x 10 <sup>-2</sup>	1.23	0.00120	342		
1.20	4.15	2.91	0.0170	5.842 x 10 <sup>-3</sup>	3.94	0.0997	2.530 x 10 <sup>-2</sup>	2.58	0.00220	391		

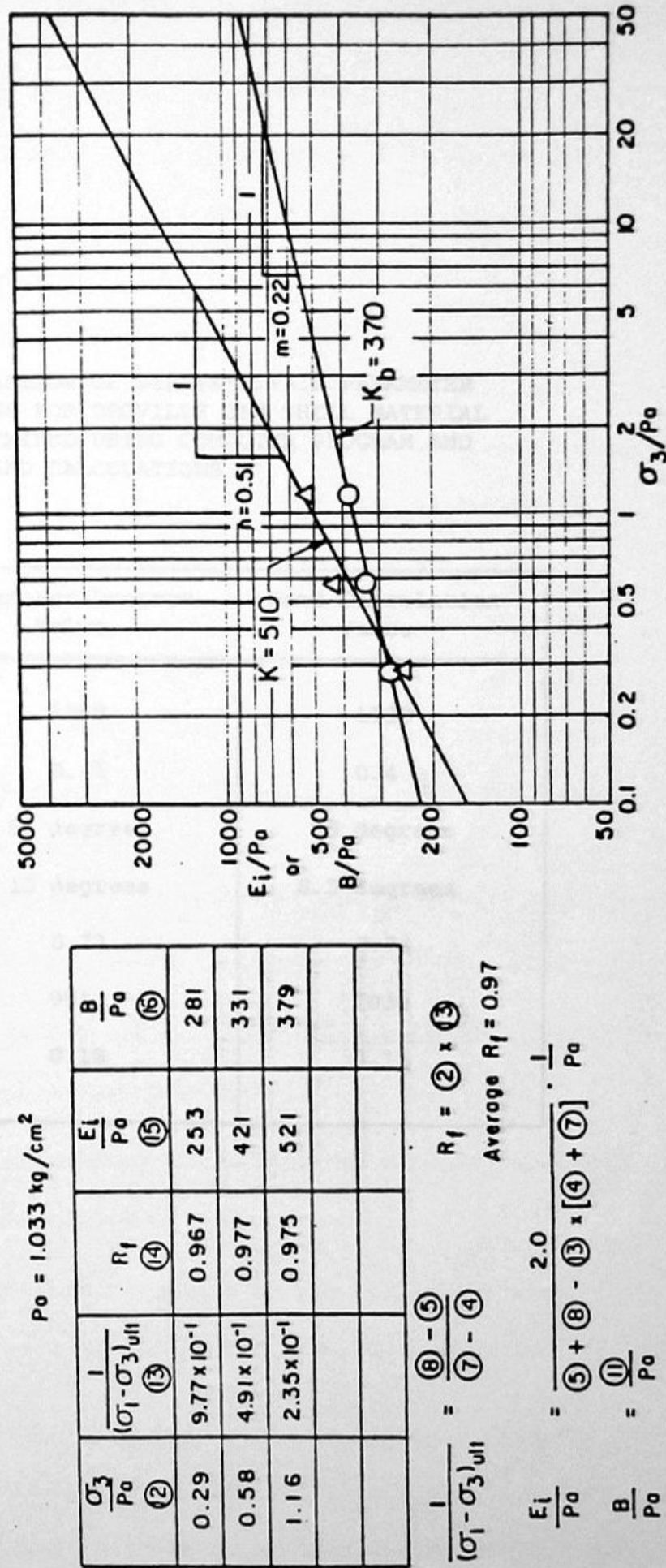


Fig. 24 EXAMPLE OF DETERMINATION OF HYPERBOLIC PARAMETERS FOR MONTEREY NO. 0 SAND. (SP - 17B)

COMPARISON OF PARAMETER VALUES

The stress-strain and strength characteristics of soils, and the values of the hyperbolic parameters, vary over wide ranges depending on the soil type and test conditions. For purposes of judging the values of parameters estimated from laboratory test data, the following table compares values determined by hand calculations with those determined by computer program.

**TABLE 3. COMPARISON OF STRESS-STRAIN PARAMETER VALUES FOR OROVILLE DAM SHELL MATERIAL DETERMINED USING COMPUTER PROGRAM AND BY HAND CALCULATIONS**

Parameter	Computer Program Value	Hand Calculation Value
K	1289	1320
n	0.41	0.4
$\phi$	55 degrees	55 degrees
$\Delta\phi$	10 degrees	8.5 degrees
$R_f$	0.73	0.73
$K_b$	991	1030
m	0.18	0.15

### COMPILATIONS OF PARAMETER VALUES

The stress-strain and strength characteristics of soils, and the values of the hyperbolic parameters, vary over wide ranges depending on the soil type and test conditions. For purposes of judging the values of parameters calculated from laboratory test data, or for estimating values of the parameters when insufficient test data are available for their determination, it is useful to have available values of the parameters for similar soils under the same test conditions.

Using data from theses, research reports, engineering reports, and published papers, parameter values have been determined for about 135 different soils. Some of these data have been judged to be inconsistent or unreliable and have therefore been omitted from this report. Data are summarized in Tables 5 and 6 for 80 soils for which the data were considered to be of the highest quality and the greatest dependency.

These compilations have been found to be useful in three ways:

- (1) For purposes of judging the reliability of parameter values determined from laboratory test data.
- (2) For purposes of determining the effects of various factors which influence the values of the parameters.
- (3) For purposes of estimating values of the parameters when insufficient data are available for their determination.

Parameters for Soils Tested Under Drained Conditions. Data for 41 soils tested under drained conditions are listed in Table 5, and an explanation of the headings used in Table 5 is contained in Table 4. The

TABLE 4. EXPLANATION OF COLUMN HEADINGS IN TABLES 5 AND 6

Heading	Explanation
Soil	Classification according to Unified System
Group	Identifying number
Soil Description	Origin and characteristics of soil
References	Publications from which data were obtained
D <sub>60</sub> , D <sub>30</sub> , D <sub>10</sub>	60%, 30%, and 10% sizes in mm
LL	Liquid Limit
PI	Plasticity Index
Compaction Type	Compaction procedure--Standard AASHO, Harvard kneading, or energy in ft-lbs per cubic ft
Maximum dry unit weight	Maximum dry unit weight as determined by the compaction test used (lb/ft <sup>3</sup> )
Optimum water content	Optimum water content in the compaction test used (% of dry weight)
Dry unit weight	Initial dry unit weight of test specimens (lb/ft <sup>3</sup> )
Water Content	Initial water content of test specimens (% of dry weight)
Initial Void Ratio	Void ratio of test specimen at beginning of test
Relative Density	$D_r = (e_{loose} - e) / (e_{loose} - e_{dense})$
Degree of Saturation	Initial degree of saturation
Rating	Estimated consistency and reliability of data, judged by comparing stress-strain and volume change curves calculated using the listed parameters with the experimental curves. *** = Excellent, ** = Very Good, * = Good. Data of lesser quality were discarded.
Particle Shape	Average particle shape as described in reference
Stress Range	Range of values of σ <sub>3</sub> used in tests (tons/ft <sup>2</sup> )

TABLE 4. (CONTINUED)

Heading	Explanation
Number of tests	Number of tests used in evaluating the stress-strain parameters
c	Cohesion intercept (tons/ft <sup>2</sup> )
Friction Angle	$\phi_0$ and $\Delta\phi$ ( $\Delta\phi$ in parentheses) $\phi_0$ = friction angle for $\sigma_3$ = 1 atmosphere $\Delta\phi$ = reduction in friction angle for a 10-fold increase in $\sigma_3$
K	Modulus number
n	Modulus exponent
R <sub>f</sub>	Failure ratio
K <sub>b</sub>	Bulk modulus number
m	Bulk modulus exponent

TABLE 5. STRESS-STRAIN AND STRENGTH PARAMETERS FOR SOILS TESTED UNDER DRAINED CONDITIONS

Soil Group	Soil Description	Grain Size, mm		P <sub>1</sub>	Compaction		Init. Relative Density	Degree of Saturation	Particle Shape	Strength Range (TSF) Tests	Cohesion	Friction Angle	E	n	K <sub>d</sub>	m						
		D <sub>60</sub>	D <sub>50</sub>		Type	Dry Unit Wt. (kN/m <sup>3</sup> )																
CS	Conglomerate Rockfill (Inertial, Dens.)	47.	7.5	0.9		116.9	0.39	90	**	Sub-angular	1.3-25.5	3	0-	50 (10)	540	.43	.64	135	.24			
CS	Granitic Gneiss Rockfill (Dens.)	79.	24.	4.		123.7	0.32	95	**	Sub-angular	1.3-25.6	3	0-	44 (9)	210	.51	.60	100	.24			
CS	Quartzite Rockfill (Furnace-Dam Shell)	10.	-	-					**	Sub-angular	4.1-36.9	4	0-	49 (6)	540	.48	.65	320	.23			
CS	Quartzite Rockfill (Furnace-Dam Shell)	25.	-	-					**	Sub-rounded	4.1-36.9	4	0-	51 (7)	950	.52	.59	470	.23			
CS	Quartzite Rockfill (Furnace-Dam Shell)	10.	-	-					**	Sub-rounded	4.1-36.9	4	0-	51 (7)	690	.45	.59	360	.23			
CS	Quartzite Rockfill (Furnace-Dam Shell)	10.	-	-					**	Sub-rounded	4.1-36.9	4	0-	51 (8)	690	.45	.59	370	.23			
CS	Furnace-Dam Gravel	21.	2.	0.25		132.1	0.34	65	**	Sub-rounded	4.1-36.9	6	0-	51 (9)	690	.45	.59	170	.23			
CS	Gloria Rockfill (El Infanteville Dam)	93.	42.	17.		105.2	0.56	50	**	Angular	4-17.0	7	0-	46 (9)	340	.28	.71	52	.18			
CS	Gloria Rockfill (El Infanteville Dam)	22.	1.2	0.23		105.2	0.5	50	**	Angular	5.1-25.5	3	0-	41 (8)	420	.50	.71	255	.18			
CS	Sandy Gravel (Mica Dam Site)	19.	2.6	1.		133.8	0.3	95	**	Angular	5.1-25.6	3	0-	52 (10)	450	.37	.61	255	.18			
CS	Sabatini Rockfill (Pyramid Dam Shell)	4.1	1.8	0.6		148.0	0.21	100	**	Angular	5.0-16.0	4	0-	53 (8)	1300	.40	.72	900	.22			
CS	Silty Sandy Gravel (Orovilles Dam)	18.	4.8	0.4	21	152.0	0.21	100	**	Angular	1.2-18.6	4	0-	51 (8)	1780	.39	.67	1300	.16			
CS	Silty Sandy Gravel (Orovilles Dam Small)	13.2	4.6	0.36		152.0	0.2	100	**	Angular	1.2-18.6	4	0-	51 (8)	1780	.39	.67	1300	.16			
CS	Angular Gravel (Orovilles Dam Small)	15.	12.	6.		99.0	3.2	99	**	Angular	2.0-14.1	3	0-	51 (8)	410	.21	.71	395	.17			
CS	Crushed Basaltic Brick (Round Butte Dam)	Shannon & Wilson (44)	-	-					**	Angular	1.8-10.8	4	0-	50 (10)	2500	.21	.75	1600	0			
CS	Crushed Basaltic Brick (Round Butte Dam)	Brougham (5)	10.	3.	0.6		113.0	10.8	223	**	Angular	1.8-12.5	3	0-	49 (9)	990	.28	.73	600	0		
CS	Sandy Gravel (Mica Dam Core)	Bird (1)	12.	0.6		107.0	10.8	100	51	Angular	1.1-4.3	4	0-	44 (8)	420	.50	.72	600	0			
CS	Sabatini Rockfill (Pyramid Dam Shell)	Marschall (27)	4.1	1.8	0.6		111.6	0.46	100	**	Angular	1.2-16.0	4	0-	53 (9)	1600	.08	.72	600	0		
CS	Sabatini Rockfill (Pyramid Dam Shell)	Marschall (27)	4.1	1.8	0.6		140.7	0.43	190	**	Angular	2.2-46.0	4	0-	55 (10)	1000	.22	.70	380	.14		
CS	Sabatini Rockfill (Pyramid Dam Shell)	Marschall (27)	4.1	1.8	0.6		140.7	0.43	190	**	Angular	2.0-46.0	4	0-	53 (10)	260	.50	.76	100	.15		
CS	Sabatini Rockfill (Pyramid Dam Shell)	Marschall (27)	4.1	1.8	0.6		140.7	0.43	190	**	Angular	2.2-46.0	4	0-	43 (10)	320	.46	.51	110	.16		
CS	Sabatini Rockfill (Pyramid Dam Shell)	Marschall (27)	4.1	1.8	0.6		140.7	0.43	190	**	Angular	1.0-11.1	4	0-	44 (10)	1900	.50	.67	180	.16		
CS	Sabatini Rockfill (Pyramid Dam Shell)	Marschall (27)	4.1	1.8	0.6		140.7	0.43	190	**	Angular	1.0-11.1	4	0-	35 (11)	430	.27	.64	230	.03		
CS	Sabatini Rockfill (Pyramid Dam Shell)	Marschall (27)	4.1	1.8	0.6		140.7	0.43	190	**	Angular	1.0-11.1	4	0-	35 (11)	430	.27	.64	230	.03		
CS	Veneto Sandstone (0.5 in. Max. size)	Becker, Chan & Seidl (12)	0.17	0.07	0.025	MP	MP	16,450	120.0	13.2	108.7	13.5	0.47	93	**	Sub-rounded	1.0-11.1	4	0-	4500	0	
CS	Glacial Cretaceous Sand	Bishop (4)	0.03	0.03	0.034	MP	MP	118.3	117.5	0.47	93	**	Sub-rounded	1.0-11.1	4	0-	44 (10)	1900	.50	.67	180	.16
CS	Glacial Cretaceous Sand	Bishop (4)	0.03	0.03	0.034	MP	MP	118.3	117.5	0.47	93	**	Sub-rounded	1.0-11.1	4	0-	44 (10)	1900	.50	.67	180	.16
CS	Sacramento River Sand	Lane (14)	0.22	0.17	0.15	MP	MP	108.5	112.3	0.5	80	**	Sub-rounded	1.0-11.1	4	0-	44 (10)	1900	.50	.67	180	.16
CS	Sacramento River Sand	Lane (14)	0.22	0.17	0.15	MP	MP	108.5	112.3	0.5	80	**	Sub-rounded	1.0-11.1	4	0-	44 (10)	1900	.50	.67	180	.16
CS	Sacramento River Sand	Lane (14)	0.22	0.17	0.15	MP	MP	108.5	112.3	0.5	80	**	Sub-rounded	1.0-11.1	4	0-	44 (10)	1900	.50	.67	180	.16
CS	Sacramento River Sand	Lane (14)	0.22	0.17	0.15	MP	MP	108.5	112.3	0.5	80	**	Sub-rounded	1.0-11.1	4	0-	44 (10)	1900	.50	.67	180	.16
CS	Sacramento River Sand	Lane (14)	0.22	0.17	0.15	MP	MP	108.5	112.3	0.5	80	**	Sub-rounded	1.0-11.1	4	0-	44 (10)	1900	.50	.67	180	.16
CS	Sacramento River Sand	Lane (14)	0.22	0.17	0.15	MP	MP	108.5	112.3	0.5	80	**	Sub-rounded	1.0-11.1	4	0-	44 (10)	1900	.50	.67	180	.16
CS	Sacramento River Sand	Lane (14)	0.22	0.17	0.15	MP	MP	108.5	112.3	0.5	80	**	Sub-rounded	1.0-11.1	4	0-	44 (10)	1900	.50	.67	180	.16
CS	Sacramento River Sand	Lane (14)	0.22	0.17	0.15	MP	MP	108.5	112.3	0.5	80	**	Sub-rounded	1.0-11.1	4	0-	44 (10)	1900	.50	.67	180	.16
CS	Sacramento River Sand	Lane (14)	0.22	0.17	0.15	MP	MP	108.5	112.3	0.5	80	**	Sub-rounded	1.0-11.1	4	0-	44 (10)	1900	.50	.67	180	.16
CS	Sacramento River Sand	Lane (14)	0.22	0.17	0.15	MP	MP	108.5	112.3	0.5	80	**	Sub-rounded	1.0-11.1	4	0-	44 (10)	1900	.50	.67	180	.16
CS	Sacramento River Sand	Lane (14)	0.22	0.17	0.15	MP	MP	108.5	112.3	0.5	80	**	Sub-rounded	1.0-11.1	4	0-	44 (10)	1900	.50	.67	180	.16
CS	Sacramento River Sand	Lane (14)	0.22	0.17	0.15	MP	MP	108.5	112.3	0.5	80	**	Sub-rounded	1.0-11.1	4	0-	44 (10)	1900	.50	.67	180	.16
CS	Sacramento River Sand	Lane (14)	0.22	0.17	0.15	MP	MP	108.5	112.3	0.5	80	**	Sub-rounded	1.0-11.1	4	0-	44 (10)	1900	.50	.67	180	.16
CS	Sacramento River Sand	Lane (14)	0.22	0.17	0.15	MP	MP	108.5	112.3	0.5	80	**	Sub-rounded	1.0-11.1	4	0-	44 (10)	1900	.50	.67	180	.16
CS	Sacramento River Sand	Lane (14)	0.22	0.17	0.15	MP	MP	108.5	112.3	0.5	80	**	Sub-rounded	1.0-11.1	4	0-	44 (10)	1900	.50	.67	180	.16
CS	Sacramento River Sand	Lane (14)	0.22	0.17	0.15	MP	MP	108.5	112.3	0.5	80	**	Sub-rounded	1.0-11.1	4	0-	44 (10)	1900	.50	.67	180	.16
CS	Sacramento River Sand	Lane (14)	0.22	0.17	0.15	MP	MP	108.5	112.3	0.5	80	**	Sub-rounded	1.0-11.1	4	0-	44 (10)	1900	.50	.67	180	.16
CS	Sacramento River Sand	Lane (14)	0.22	0.17	0.15	MP	MP	108.5	112.3	0.5	80	**	Sub-rounded	1.0-11.1	4	0-	44 (10)	1900	.50	.67	180	.16
CS	Sacramento River Sand	Lane (14)	0.22	0.17	0.15	MP	MP	108.5	112.3	0.5	80	**	Sub-rounded	1.0-11.1	4	0-	44 (10)	1900	.50	.67	180	.16
CS	Sacramento River Sand	Lane (14)	0.22	0.17	0.15	MP	MP	108.5	112.3	0.5	80	**	Sub-rounded	1.0-11.1	4	0-	44 (10)	1900	.50	.67	180	.16
CS	Sacramento River Sand	Lane (14)	0.22	0.17	0.15	MP	MP	108.5	112.3	0.5	80	**	Sub-rounded	1.0-11.1	4	0-	44 (10)	1900	.50	.67	180	.16
CS	Sacramento River Sand	Lane (14)	0.22	0.17	0.15	MP	MP	108.5	112.3	0.5	80	**	Sub-rounded	1.0-11.1	4	0-	44 (10)	1900	.50	.67	180	.16
CS	Sacramento River Sand	Lane (14)	0.22	0.17	0.15	MP	MP	108.5	112.3	0.5	80	**	Sub-rounded	1.0-11.1	4	0-	44 (10)	1900	.50	.67	180	.16
CS	Sacramento River Sand	Lane (14)	0.22	0.17	0.15	MP	MP	108.5	112.3	0.5	80	**	Sub-rounded	1.0-11.1	4	0-	44 (10)	1900	.50	.67	180	.16
CS	Sacramento River Sand	Lane (14)	0.22	0.17	0.15	MP	MP	108.5	112.3	0.5	80	**	Sub-rounded	1.0-11.1	4	0-	44 (10)	1900	.50	.67	180	.16
CS	Sacramento River Sand	Lane (14)	0.22	0.17	0.15	MP	MP	108.5	112.3	0.5	80	**	Sub-rounded	1.0-11.1	4	0-	44 (10)	1900	.50	.67	180	.16
CS	Sacramento River Sand	Lane (14)	0.22	0.17	0.15	MP	MP	108.5	112.3	0.5	80	**	Sub-rounded	1.0-11.1	4	0-	44 (10)	1900	.50	.67	180	.16
CS	Sacramento River Sand	Lane (14)	0.22	0.17	0.15	MP	MP	108.5	112.3	0.5	80	**	Sub-rounded	1.0-11.1	4	0-	44 (10)	1900	.50	.67	180	.16
CS	Sacramento River Sand	Lane (14)	0.22	0.17	0.15	MP	MP	108.5	112.3	0.5	80	**	Sub-rounded	1.0-11.1	4	0-	44 (10)	1900	.50	.67	180	.16
CS	Sacramento River Sand	Lane (14)	0.22	0.17	0.15	MP	MP	108.5	112.3	0.5	80	**	Sub-rounded	1.0-11.1	4	0-	44 (10)	1900	.50	.67	180	.16
CS	Sacramento River Sand	Lane (14)	0.22	0.17	0.15	MP	MP															

TABLE 6. STRESS-STRAIN AND STRENGTH PARAMETERS FOR SOILS TESTED UNDER UNCONSOLIDATED-UNDRAINED CONDITIONS

TABLE 6. (CONTINUED)

Soil Group	Soil Description	References		Grain Size, mm		Compaction						Degree of Saturation	Stress Range (TSP)	Number of Tests	C	Friction Angle	K	n	R <sub>f</sub>	K <sub>D</sub>			
		I60	D30	010	IL	PI	Type	Unit Wt.	w/c	(FCP)	Dry Opt.												
CL-11C	Sandy Clay (Somerville Date)	CORE, Fort Worth District (15)	0.06	0.002	-	25	12	Std. AASHO	107.5	16.8	102.6	19.3	87	-	-5- 6.0	4	.74	6	23	.32	.61		
CL-11D	Sandy Clay (Somerville Date)	CORE, Fort Worth District (15)	0.06	0.002	-	25	12	Std. AASHO	107.5	16.8	106.7	16.7	85	-	-5- 6.0	4	.91	18	260	.60	.93		
CL-11E	Sandy Clay (Somerville Date)	CORE, Fort Worth District (15)	0.06	0.002	-	25	12	Std. AASHO	107.5	16.8	101.5	16.3	72	-	-5- 6.0	4	.66	20	220	.23	.90		
CL-12A	Sandy Clay (Somerville Date)	CORE, Fort Worth District (15)	0.065	0.0055	0.001	38	25	Std. AASHO	106.1	17.2	105.0	18.6	89	-	-5- 6.0	4	1.30	8	140	.20	.84		
CL-12C	Sandy Clay (Somerville Date)	CORE, Fort Worth District (15)	0.065	0.0055	0.001	38	25	Std. AASHO	106.1	17.2	101.9	17.1	75	-	-5- 6.0	4	1.00	13	120	.47	.83		
CL-12D	Sandy Clay (Somerville Date)	CORE, Fort Worth District (15)	0.065	0.0055	0.001	38	25	Std. AASHO	106.1	17.2	103.0	19.7	69	-	-5- 6.0	4	.80	2	47	.33	.82		
CL-12E	Sandy Clay (Somerville Date)	CORE, Fort Worth District (15)	0.065	0.0055	0.001	38	25	Std. AASHO	106.1	17.2	106.5	13.9	70	-	-5- 6.0	4	1.30	24	950	-.15	.90		
CL-12F	Sandy Clay (Somerville Date)	CORE, Fort Worth District (15)	0.065	0.0055	0.001	38	25	Std. AASHO	106.1	17.2	108.3	16.9	69	-	-5- 6.0	4	1.50	8	470	0.	.95		
CL-12G	Sandy Clay (Somerville Date)	CORE, Fort Worth District (15)	0.065	0.0055	0.001	38	25	Std. AASHO	104.9	17.6	98.7	20.8	86	-	-5- 6.0	4	.67	4	75	.44	.88		
CL-12H	Sandy Clay (Somerville Date)	CORE, Fort Worth District (15)	0.065	0.0045	-	36	23	Std. AASHO	104.9	17.6	104.9	14.8	72	-	-5- 6.0	4	1.80	23	840	-.19	.84		
CL-12I	Sandy Clay (Somerville Date)	CORE, Fort Worth District (15)	0.065	0.0045	-	36	23	Std. AASHO	104.9	17.6	102.0	11.4	76	-	-5- 6.0	4	1.20	12	270	.06	.87		
CL-12J	Sandy Clay (Somerville Date)	CORE, Fort Worth District (15)	0.065	0.0045	-	36	23	Std. AASHO	104.9	17.6	100.5	14.2	62	-	-5- 6.0	4	1.40	29	1100	-.36	.83		
CL-13E	Sandy Clay (Somerville Date)	CORE, Fort Worth District (15)	0.046	0.0045	-	36	23	Std. AASHO	104.9	17.6	104.4	14.8	72	-	-5- 6.0	4	1.80	23	840	-.19	.84		
CL-13F	Sandy Clay (Somerville Date)	CORE, Fort Worth District (15)	0.046	0.0045	-	36	23	Std. AASHO	104.9	17.6	101.5	14.2	62	-	-5- 6.0	4	1.40	29	1100	-.36	.83		
CL-13G	Sandy Clay (Somerville Date)	CORE, Fort Worth District (15)	0.046	0.0045	-	36	23	Std. AASHO	104.9	17.6	106.5	13.9	70	-	-5- 6.0	4	1.30	24	950	-.15	.90		
CL-13H	Sandy Clay (Somerville Date)	CORE, Fort Worth District (15)	0.046	0.0045	-	36	23	Std. AASHO	104.9	17.6	108.3	16.9	69	-	-5- 6.0	4	1.50	8	470	0.	.95		
CL-13I	Sandy Clay (Somerville Date)	CORE, Fort Worth District (15)	0.046	0.0045	-	36	23	Std. AASHO	104.9	17.6	98.7	20.8	86	-	-5- 6.0	4	.67	4	75	.44	.88		
CL-13L	Sandy Clay (Somerville Date)	CORE, Fort Worth District (15)	0.046	0.0045	-	36	23	Std. AASHO	104.9	17.6	104.9	14.8	72	-	-5- 6.0	4	1.80	23	840	-.19	.84		
CL-13M	Sandy Clay (Somerville Date)	CORE, Fort Worth District (15)	0.046	0.0045	-	36	23	Std. AASHO	104.9	17.6	102.0	11.4	76	-	-5- 6.0	4	1.20	12	270	.06	.87		
CL-13N	Sandy Clay (Somerville Date)	CORE, Fort Worth District (15)	0.046	0.0045	-	36	23	Std. AASHO	104.9	17.6	100.5	14.2	62	-	-5- 6.0	4	1.40	29	1100	-.36	.83		
CL-13O	Sandy Clay (Somerville Date)	CORE, Fort Worth District (15)	0.046	0.0045	-	36	23	Std. AASHO	104.9	17.6	104.4	14.8	72	-	-5- 6.0	4	1.80	23	840	-.19	.84		
CL-13P	Sandy Clay (Somerville Date)	CORE, Fort Worth District (15)	0.046	0.0045	-	36	23	Std. AASHO	104.9	17.6	101.0	20.1	99.1	-	-5- 6.0	3	1.40	13	410	.15	.87		
CL-13Q	Sandy Clay (Somerville Date)	CORE, Fort Worth District (15)	0.046	0.0045	-	36	23	Std. AASHO	104.9	17.6	104.4	17.5	84	-	-5- 6.0	3	1.77	2	57	.43	.86		
CL-13R	Sandy Clay (Somerville Date)	CORE, Fort Worth District (15)	0.046	0.0045	-	36	23	Std. AASHO	105.0	20.2	98.0	92	91	-	1.0- 3.0	2	.97	1	110	.43	.90		
CL-13S	Sandy Clay (Somerville Date)	CORE, Fort Worth District (15)	0.046	0.0045	-	36	23	Std. AASHO	105.0	20.2	99.7	22.9	91	-	1.0- 3.0	2	1.0- 3.0	2	.97	1	110	.43	.90
CL-13T	Sandy Clay (Somerville Date)	CORE, Fort Worth District (15)	0.046	0.0045	-	36	23	Std. AASHO	105.0	20.2	100.0	20.1	99.1	-	2.0- 6.0	3	1.10	2	100	.10	.87		
CL-13U	Sandy Clay (Somerville Date)	CORE, Fort Worth District (15)	0.046	0.0045	-	36	23	Std. AASHO	105.0	20.2	101.0	20.1	98.1	-	2.0- 6.0	3	1.10	2	100	.10	.87		
CL-14	Lean Clay (Clinton Date)	CORE, Kansas City District (17)	-	-	-	46	27	Std. AASHO	101.0	21.1	98.0	22.7	90	-	1.0- 5.0	3	1.40	13	410	.15	.87		
CL-14C	Lean Clay (Clinton Date)	CORE, Kansas City District (17)	-	-	-	37	18	Std. AASHO	101.0	21.1	99.7	22.9	91	-	1.0- 5.0	3	1.77	2	57	.43	.86		
CL-14D	Lean Clay (Clinton Date)	CORE, Kansas City District (17)	-	-	-	43	24	Std. AASHO	101.0	20.1	99.1	22.7	90	-	1.0- 5.0	3	1.99	1	110	.43	.90		
CL-14E	Lean Clay (Clinton Date)	CORE, Kansas City District (17)	-	-	-	43	24	Std. AASHO	101.0	20.1	98.9	22.7	90	-	2.0- 6.0	3	1.10	2	100	.10	.87		
CL-14F	Lean Clay (Clinton Date)	CORE, Kansas City District (17)	-	-	-	43	24	Std. AASHO	101.0	20.1	98.1	21.9	90	-	2.0- 6.0	3	1.10	2	100	.10	.87		
CL-14G	Lean Clay (Clinton Date)	CORE, Kansas City District (17)	-	-	-	43	24	Std. AASHO	101.0	20.1	97.6	22.7	83	-	2.0- 6.0	3	1.78	2	53	.41	.85		
CL-14H	Lean Clay (Clinton Date)	CORE, Kansas City District (17)	-	-	-	43	24	Std. AASHO	101.0	20.1	97.6	22.7	83	-	2.0- 6.0	3	1.78	2	53	.41	.85		
CL-14I	Lean Clay (Clinton Date)	CORE, Kansas City District (17)	-	-	-	34	18	Std. AASHO	113.0	15.1	107.4	18.1	86	-	6.0-10.0	2	1.20	0	240	0.	.93		
CL-14J	Lean Clay (Clinton Date)	CORE, Kansas City District (17)	-	-	-	34	18	Std. AASHO	113.0	15.1	107.4	18.1	86	-	6.0-10.0	2	1.20	0	240	0.	.93		
CL-14K	Lean Clay (Clinton Date)	CORE, Kansas City District (17)	-	-	-	34	19	Harvard	115.0	14.6	114.0	12.2	72	-	1.5- 6.0	2	1.60	12	150	.16	.79		
CL-14L	Lean Clay (Clinton Date)	CORE, Kansas City District (17)	-	-	-	34	19	Harvard	116.2	15.2	110.9	13.0	67	-	1.0-14.3	5	2.00	20	440	.17	.85		
CL-14M	Lean Clay (Clinton Date)	CORE, Kansas City District (17)	-	-	-	34	19	Harvard	116.2	15.2	115.8	13.1	77	-	1.0-14.3	4	2.50	20	440	.34	.86		
CL-14N	Lean Clay (Clinton Date)	CORE, Kansas City District (17)	-	-	-	34	19	Harvard	116.2	15.2	115.8	13.1	77	-	1.0-14.3	4	2.50	20	440	.34	.86		
CL-14O	Lean Clay (Clinton Date)	CORE, Kansas City District (17)	-	-	-	34	19	Harvard	116.2	15.2	115.8	13.1	77	-	1.0-14.3	4	2.50	20	440	.34	.86		
CL-14P	Lean Clay (Clinton Date)	CORE, Kansas City District (17)	-	-	-	34	19	Harvard	116.2	15.2	115.8	13.1	77	-	1.0-14.3	4	2.50	20	440	.34	.86		
CL-14Q	Lean Clay (Clinton Date)	CORE, Kansas City District (17)	-	-	-	34	19	Harvard	116.2	15.2	115.8	13.1	77	-	1.0-14.3	4	2.50	20	440	.34	.86		
CL-14R	Lean Clay (Clinton Date)	CORE, Kansas City District (17)	-	-	-	34	19	Harvard	116.2	15.2	115.8	13.1	77	-	1.0-14.3	4	2.50	20	440	.34	.86		
CL-14S	Lean Clay (Clinton Date)	CORE, Kansas City District (17)	-	-	-	34	19	Harvard	116.2	15.2	115.8	13.1	77	-	1.0-14.3	4	2.50	20	440	.34	.86		
CL-14T	Lean Clay (Clinton Date)	CORE, Kansas City District (17)	-	-	-	34	19	Harvard	116.2	15.2	115.8	13.1	77	-	1.0-14.3	4	2.50	20	440	.34	.86		
CL-14U	Lean Clay (Clinton Date)	CORE, Kansas City District (17)	-	-	-	34	19	Harvard	116.2	15.2	115.8	13.1	77	-	1.0-14.3	4	2.50	20	440	.34	.86		
CL-14V	Lean Clay (Clinton Date)	CORE, Kansas City District (17)	-	-	-	34	19	Harvard	116.2	15.2	115.8	13.1	77	-	1.0-14.3	4	2.50	20	440	.34	.86		
CL-14W	Lean Clay (Clinton Date)	CORE, Kansas City District (17)	-	-	-	34	19	Harvard	116.2	15.2	115.8	13.1	77	-	1.0-14.3	4	2.50	20	440	.34	.86		
CL-14X	Lean Clay (Clinton Date)	CORE, Kansas City District (17)	-	-	-	34	19	Harvard	116.2	15.2	115.8	13.1	77	-	1.0-14.3	4	2.50	20	440	.34	.86		
CL-14Y	Lean Clay (Clinton Date)	CORE, Kansas City District (17)	-	-	-	34	19	Harvard	116.2	15.2	115.8	13.1	77	-	1.0-14.3	4	2.50	20	440	.34	.86		
CL-14Z	Lean Clay (Clinton Date)	CORE, Kansas City District (17)	-	-	-	34	19	Harvard	116.2	15.2	115.8	13.1	77	-	1.0-14.3	4	2.50	20	440	.34	.86		
CL-14AA	Lean Clay (Clinton Date)	CORE, Kansas City District (17)	-	-	-	34	19	Harvard	116.2	15.2	115.8	13.1	77	-	1.0-14.3	4	2.50	20	440	.34	.86		
CL-14AB	Lean Clay (Clinton Date)	CORE, Kansas City District (17)	-	-	-	34	19	Harvard	116.2	15.2	115.8	13.1	77	-	1.0-14.3	4	2.50	20	440	.34	.86		
CL-14AC	Lean Clay (Clinton Date)	CORE, Kansas City District (17)	-	-	-	34	19	Harvard	116.2	15.2	115.8	13.1	77	-	1.0-14.3	4	2.50	20	440	.34	.86		
CL-14AD	Lean Clay (Clinton Date)	CORE, Kansas City District (17)	-	-	-	34	19	Harvard	116.2	15.2	115.8	13.1	77	-	1.0-14.3	4	2.50	20	440	.34	.86		
CL-14AE	Lean Clay (Clinton Date)	CORE, Kansas City District (17)	-	-	-	34	19	Harvard	116.2	15.2	115.8	13.1	77	-	1.0-14.3	4	2.50	20	440	.34	.86		
CL-14AF	Lean Clay (Clinton Date)	CORE, Kansas City District (17)	-	-	-	34	19	Harvard	116.2	15.2	115.8	13.1	77	-	1.0-14.3	4	2.50	20	440	.34	.86		
CL-14AG	Lean Clay (Clinton Date)	CORE, Kansas City District (17)	-	-	-	34	19	Harvard	116.2	15.2	115.8	13.1	77	-	1.0-14.3	4	2.50	20	440	.34	.86		
CL-14AH	Lean Clay (Clinton Date)	CORE, Kansas City District (17)	-	-	-	34	19	Harvard	116.2	15.2	115.8	13.1	77	-	1.0-14.3	4	2.50	20	440	.34	.86		
CL-14AI	Lean Clay (Clinton Date)	CORE, Kansas City District (17)	-	-	-	34	19	Harvard	116.2	15.2	115.8	13.1	77	-	1.0-14.3	4	2.50	20	440	.34	.86		
CL-14AJ	Lean Clay (Clinton Date)	CORE, Kansas City District (17)	-	-	-	34																	

values of the stress-strain and strength parameters in Table 5 were calculated using the computer program in the Appendix. These values differ somewhat from the values given for the same soils by Kulhawy, Duncan and Seed (34). The differences are due to the fact that the earlier values were calculated by hand. Although the individual values differ somewhat, the differences in the stress-strain and strength behavior are not significant.

The most important factors affecting the stress-strain and strength characteristics of soils tested under drained conditions are relative density, gradation, particle shape and mineral type.

An increase in the density of a cohesionless soil will result in increased strength (higher value of  $\phi$ ), increased stiffness (higher value of  $K$ ), and increased tendency to dilate during shear (higher value of  $K_b$ ). These effects are illustrated by the tests on Sacramento River sand, which was tested at four different relative densities. For purposes of estimating the effects of changing from one relative density to another, the following approximate rules of thumb are useful:

- (1) The value of  $\phi$  increases about one degree for each 6% increase in relative density.
- (2) The value of  $\Delta\phi$  increases approximately in proportion to relative density.
- (3) The value of  $K$  increases approximately in proportion to relative density.
- (4) The value of  $K_b$  increases approximately in proportion to relative density.
- (5) The values of  $n$ ,  $m$  and  $R_f$  are not much affected by changes in relative density.

Poorly graded cohesionless soils generally have higher values of  $K$  and  $K_b$  than do well-graded cohesionless soils of the same average grain size. The values of  $\phi_o$ ,  $\Delta\phi$ ,  $n$ ,  $m$  and  $R_f$  do not appear to be related in a consistent way to gradation, at least so far as can be determined from the data in Table 5.

Rounded particles are more resistant to breakage during shear than are angular particles, and as a result soils with rounded particles tend to have higher values of  $K$ ,  $n$ ,  $K_b$  and  $m$  than do soils with angular particles, and they generally have smaller values of  $\Delta\phi$ . Values of  $\phi_o$  and  $R_f$  do not appear to be related in a consistent way to particle shape.

Parameters for Soils Tested Under Undrained Conditions. Data for 39 soils tested under unconsolidated-undrained test conditions are listed in Table 6. As noted previously for cohesionless soils, the values of the parameters were calculated using the computer program in the Appendix. They thus differ somewhat from the values published previously for the same soils by Kulhawy, Duncan, and Seed (32). The differences, however, do not represent significant differences in stress-strain and strength behavior.

The most important factors affecting the stress-strain and strength parameters of soils under unconsolidated-undrained test conditions are the Unified Soil Classification, density, water content and the structural arrangement of the soil particles which results from the soil formation process or compaction. These factors determine both the behavior in terms of effective stresses and the pore pressures which develop during undrained loading, and they therefore control the undrained stress-strain and strength behavior.

The structure of naturally occurring clayey soils is subject to disturbance during sampling, and the effects of disturbance on the values of the stress-strain and strength parameters may be very large. It is therefore essential that samples used for determining parameters for naturally occurring soils under unconsolidated-undrained test conditions be of the highest quality.

The structure of compacted soils is determined by the method of compaction and the compaction water content in relation to the optimum water content. It is therefore desirable that samples used for determining parameters for compacted soils under unconsolidated-undrained test conditions should be compacted using procedures similar to those used in the field, and it is essential that they should be compacted to the same density, and at the same water content as the soil in the field.

The values of the stress-strain and strength parameters for compacted soils can vary over an extremely wide range depending on the density and water content of the test specimens. Kulhawy, Duncan and Seed (32) presented data for Pittsburg sandy clay which illustrated the effects of density and water content. The data were obtained from tests on specimens compacted, using Harvard miniature kneading compaction equipment, to the densities and water contents shown in Fig. 25. The data for these tests have been reevaluated using the computer program in Appendix A, and the resulting values of the stress-strain and strength parameters are shown in Figs. 26 through 28.

Conservative Parameter Values. It is frequently useful to be able to estimate values of stress-strain and strength parameters for soils of

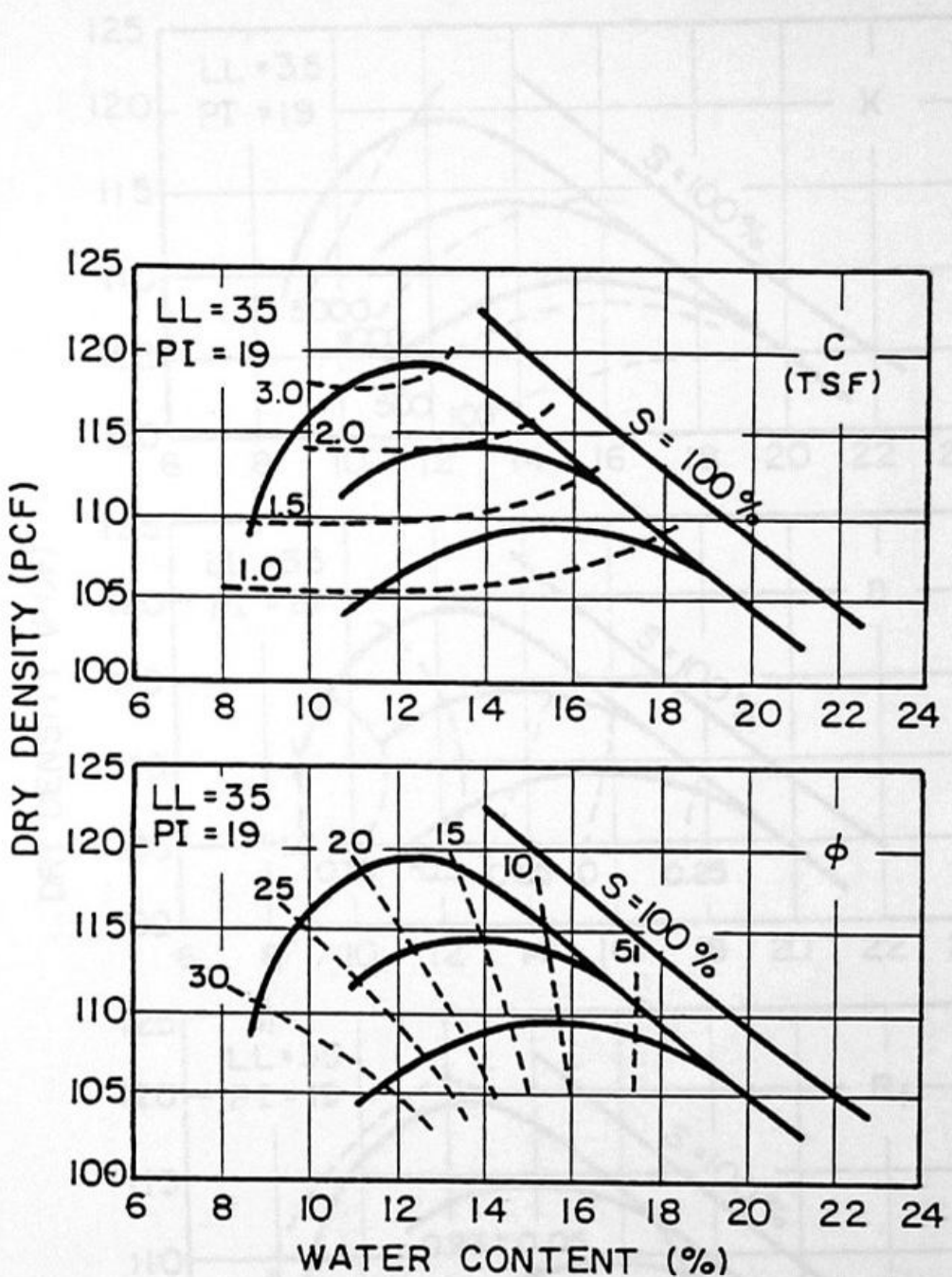


FIG. 26 STRENGTH PARAMETERS FOR COMPAKTED  
PITTSBURG SANDY CLAY TESTED UNDER  
UU TEST CONDITIONS.  
(KULHAWY, DUNCAN and SEED, 1969)

FIG. 27 MODULUS PARAMETERS FOR COMPAKTED  
PITTSBURG SANDY CLAY TESTED UNDER  
UU TEST CONDITIONS.  
(KULHAWY, DUNCAN and SEED, 1969)

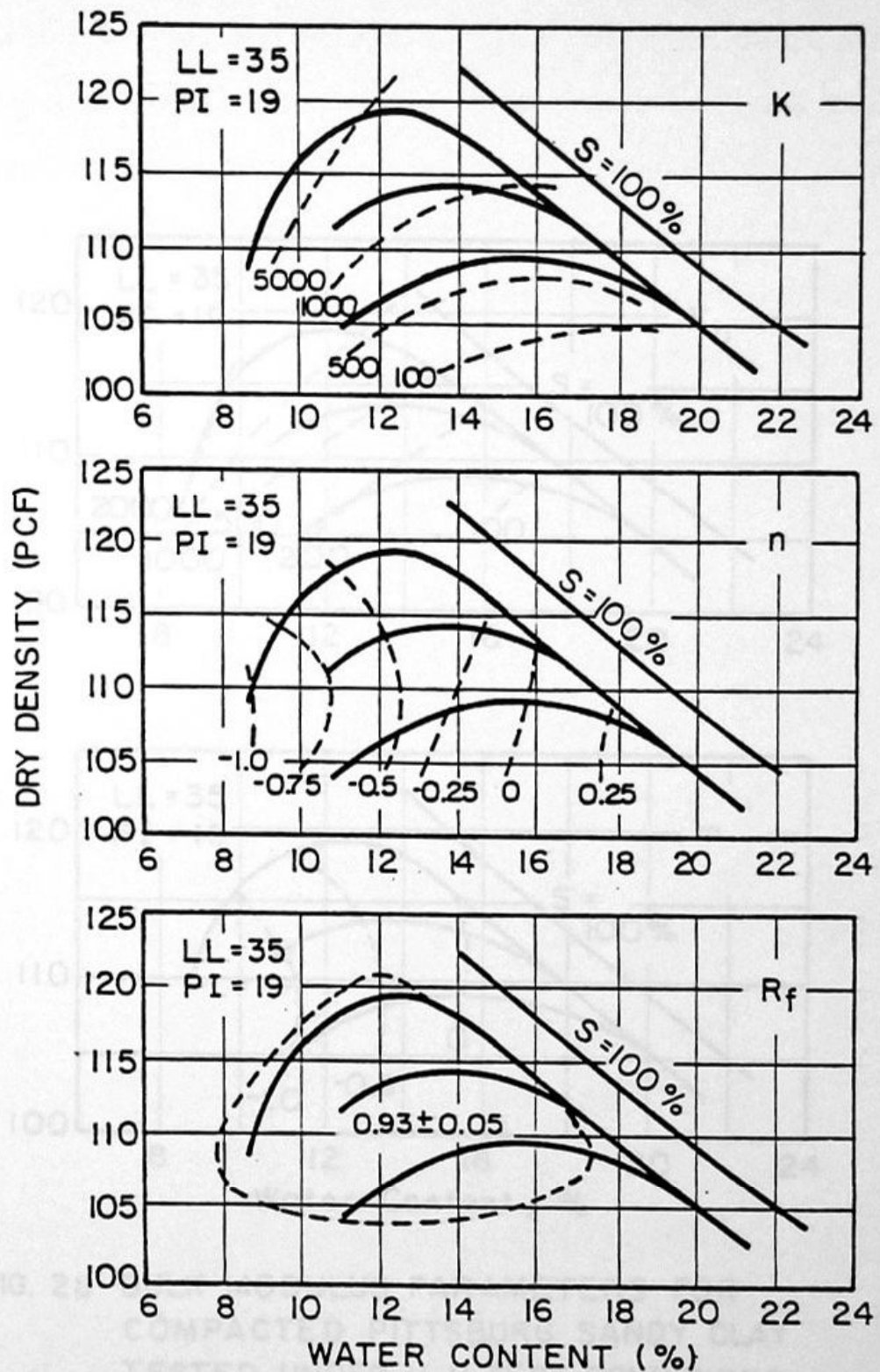


FIG. 27 MODULUS PARAMETERS FOR COMPAKTED  
PITTSBURG SANDY CLAY TESTED UNDER  
UU TEST CONDITIONS.

(KULHAWY, DUNCAN and SEED, 1969)

sample types and degree of compaction. Such estimates can be made using the compilations of data in the previous section. Until these data, compressive parameter values have been interpreted for various types of soils.

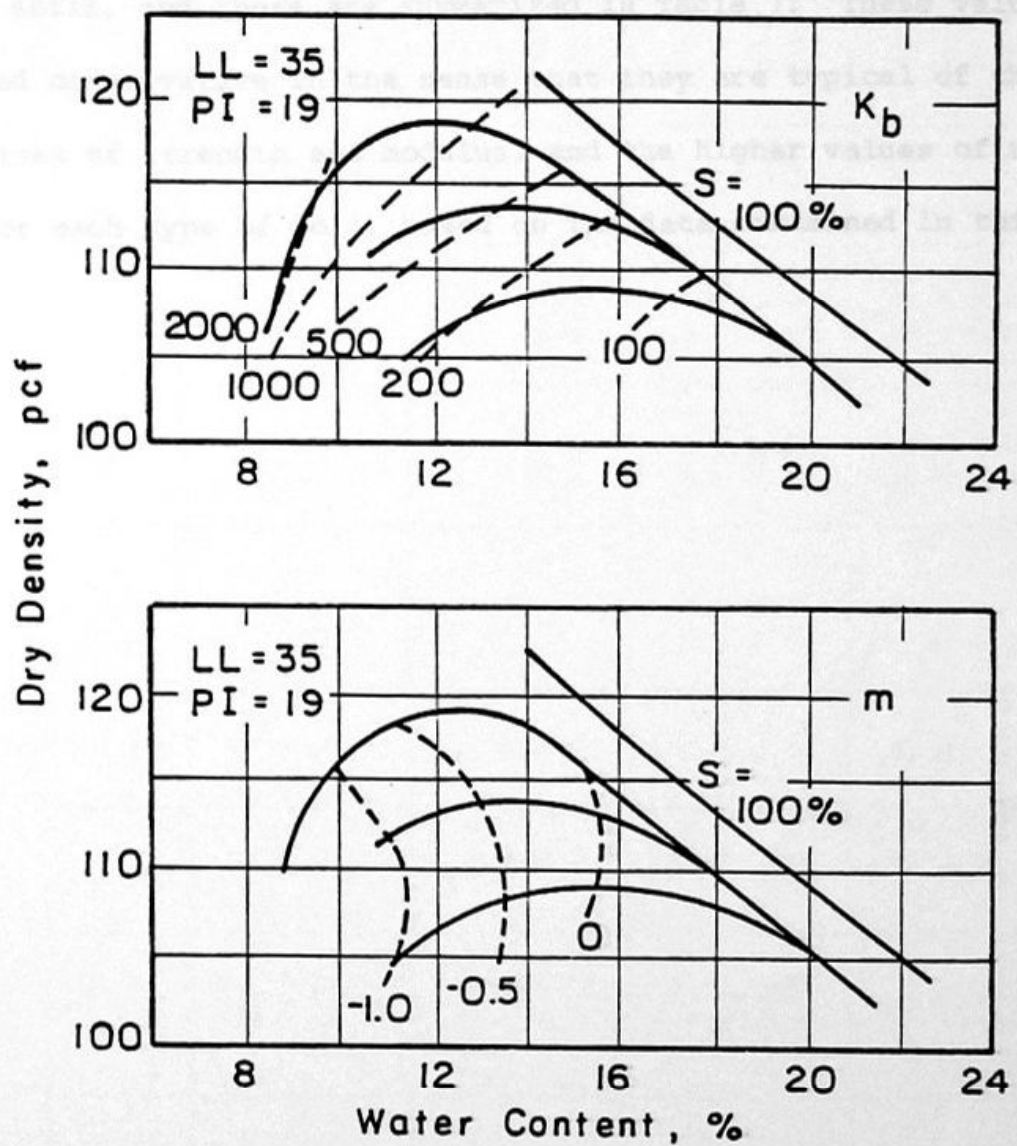


FIG. 28 BULK MODULUS PARAMETERS FOR  
COMPACTED PITTSBURG SANDY CLAY  
TESTED UNDER U-U TEST CONDITIONS.  
(CL-5).

various types and degrees of compaction. Such estimates can be made using the compilations of data in the previous section. Using these data, conservative parameter values have been interpreted for various types of soils, and these are summarized in Table 7. These values are called conservative in the sense that they are typical of the lower values of strength and modulus, and the higher values of unit weight for each type of soil, based on the data contained in this report.

TABLE 7. SOIL PROPERTIES

Unified Classification	RC Stand. AASHTO	$\gamma_m$ k/ft <sup>3</sup>	$\phi_o$ deg	$\Delta\phi$ deg	C k/ft <sup>2</sup>	k	n	R <sub>f</sub>	K <sub>b</sub>	m
GW, GP	105	0.150	42	9	0	600	0.4	0.7	175	0.2
SW, SP	100	0.145	39	7	0	450	0.4	0.7	125	0.2
	95	0.140	36	5	0	300	0.4	0.7	75	0.2
	90	0.135	33	3	0	200	0.4	0.7	50	0.2
SM	100	0.135	36	8	0	600	0.25	0.7	450	0.0
	95	0.130	34	6	0	450	0.25	0.7	350	0.0
	90	0.125	32	4	0	300	0.25	0.7	250	0.0
	85	0.120	30	2	0	150	0.25	0.7	150	0.0
SM-SC	100	0.135	33	0	0.5	400	0.6	0.7	200	0.5
	95	0.130	33	0	0.4	200	0.6	0.7	100	0.5
	90	0.125	33	0	0.3	150	0.6	0.7	75	0.5
	85	0.120	33	0	0.2	100	0.6	0.7	50	0.5
CL	100	0.135	30	0	0.4	150	0.45	0.7	140	0.2
	95	0.130	30	0	0.3	120	0.45	0.7	110	0.2
	90	0.125	30	0	0.2	90	0.45	0.7	80	0.2
	85	0.120	30	0	0.1	60	0.45	0.7	50	0.2

SUMMARY

If the results of a finite element analysis of stresses and movements in soil are to be meaningful and realistic, it is important that the stress-strain characteristics of the soil be represented in a reasonable way.

The hyperbolic stress-strain relationships described in this report can be used to represent three important characteristics of the stress-strain behavior of soils: nonlinearity, stress-dependency, and inelasticity. The values of the parameters may be determined from the results of conventional laboratory tests, and the parameters may be used for analysis of stresses and movements in stable soil masses.

The techniques used to determine values of the parameters from the results of laboratory tests are explained in detail, and compilations of parameter values are given for soils tested under both drained and unconsolidated-undrained test conditions.

ACKNOWLEDGMENT

Many people have participated in developing the concepts and the data contained in this report. The writers wish to express their appreciation for the contributions of F. H. Kulhawy, C-Y. Chang, G. W. Clough, E. S. Nobari, Poul Lade, J. M. Simon, and Antonio Soriano.

The research was sponsored by the National Science Foundation under Grant No. ENG73-08048 A02.

REFERENCES

1. Bechtel Corporation (1969) "Report on Soil Tests for the Proposed New Don Pedro Dam," San Francisco.
2. Becker, E., Chan, C. K. and Seed, H. Bolton (1972) "Strength and Deformation Characteristics of Rockfill Materials in Plane Strain and Triaxial Compression Tests," Report No. TE-72-3, Office of Research Services, University of California, Berkeley, California.
3. Bird, J. M. (1961) "Uncertainties in Earth Dam Design," Journal of the Soil Mechanics and Foundations Division, ASCE, Vol. 87, No. SM3, June, pp. 33-68.
4. Bishop, A. W. (1966) "The Strength of Soils as Engineering Materials," Geotechnique, Vol. 16, No. 2, June, pp. 89-130.
5. Broughton, N. O. (1970) "Elastic Analysis for Behavior of Rockfill," Journal of the Soil Mechanics and Foundations Division, ASCE, Sept., pp. 1715-1733.
6. Casagrande, A. and Hirschfeld, R. C. (1960) "First Progress Report on Investigation of Stress-Deformation and Strength Characteristics of Compacted Clays," Soil Mechanics Series No. 61, Harvard University, May.
7. Casagrande, A. and Hirschfeld, R. C. (1962) "Second Progress Report on Investigation of Stress-Deformation and Strength Characteristics of Compacted Clays," Soil Mechanics Series No. 65, Harvard University, April.
8. Casagrande, A., Hirschfeld, R. C. and Poulos, S. J. (1963) "Third Progress Report on Investigation of Stress-Deformation and Strength Characteristics of Compacted Clays," Soil Mechanics Series No. 70, Harvard University, November, 67 p.
9. Casagrande, A. and Poulos, S. J. (1964) "Fourth Report on Investigation of Stress-Deformation and Strength Characteristics of Compacted Clays," Soil Mechanics Series No. 74, Harvard University, October.
10. Casagrande, A. (1965) "Hohe Staudamme," Mitteilungen des Institutes fur Grundbau und Bodenmechanik, Technische Hochschule, Vienna, No. 6, December, 32 p.
11. Chang, C-Y. and Duncan, J. M. (1970) "Analysis of Soil Movements Around a Deep Excavation," Journal of Soil Mechanics and Foundations Division, ASCE, Vol. 96, No. SM5, Proc. Paper 7512, September, pp. 1655-1681.

12. Clough, G. W. (1972) "Application of the Finite Element Method to Earth-Structure Interaction," State-of-the-Art Report, Proceedings of the Symposium on Applications of the Finite Element Method in Geotechnical Engineering, U.S. Army Engineers Waterways Experiment Station, Vicksburg, Mississippi, May.
13. Clough, G. W. and Duncan, J. M. (1971) "Finite Element Analyses of Retaining Wall Behavior," Journal of the Soil Mechanics and Foundations Division, ASCE, Vol. 97, No. SM12, December.
14. Corps of Engineers, Fort Worth District (1961) "Proctor Dam: Memorandum," U.S. Department of the Army, Fort Worth District, Corps of Engineers, 1961.
15. Corps of Engineers, Fort Worth District (1961) "Somerville Dam: Design Memorandum," U.S. Department of the Army, Fort Worth District, Corps of Engineers, 1961.
16. Corps of Engineers, Jacksonville District (1964) "Rodman Dam, Cross Florida Barge Canal Project: Design Memorandum," U.S. Department of the Army, Jacksonville District, Corps of Engineers, 1964.
17. Corps of Engineers, Kansas City District (1966) "Clinton Reservoir: Design Memorandum No. 10, Supplement A, Soil Data and Embankment Design," U.S. Department of the Army, Kansas City District, Corps of Engineers, August 1967.
18. Corps of Engineers, Louisville District (1960) "Monroe Reservoir: Design Memorandum No. 2, Appendix I, Laboratory Test Data," U.S. Department of the Army, Louisville District, Corps of Engineers, February 1960.
19. Corps of Engineers, Omaha District (1968) "Chatfield Dam and Reservoir: Design Memorandum No. PC-24," U.S. Department of the Army, Omaha District, Corps of Engineers, 1968.
20. Corps of Engineers, Tulsa District (1972) "Birch Dam: Design Memorandum No. 6, Embankment, Spillway and Outlet Works," U.S. Department of the Army, Tulsa District, Corps of Engineers, September 1972.
21. Department of Water Resources (1969) "Report on Unconsolidated-Undrained Triaxial Shear Tests for the Core of Oroville Dam," State of California.
22. Duncan, J. M. and Chang, C-Y. (1970) "Nonlinear Analysis of Stress and Strain in Soils," Journal of the Soil Mechanics and Foundations Division, ASCE, Vol. 96, No. SM5, September 1970.

23. Duncan, J. M. and Clough, G. W. (1971) "Finite Element Analyses of Port Allen Lock," Journal of the Soil Mechanics and Foundations Division, ASCE, Vol. 97, No. SM8, Proc. Paper, August 1971, pp. 1053-1068.
24. Duncan, J. M. and Lefebvre, G. (1973) "Earth Pressures on Structures Due to Fault Movement," Journal of the Soil Mechanics and Foundations Division, ASCE, Vol. 99, No. SM12, Proc. Paper 10237, December 1973, pp. 1153-1163.
25. Hall, E. B. and Gordon, B. B. (1963) "Triaxial Testing with Large-Scale High Pressure Equipment," STP 361 - Laboratory Shear Testing of Soils, ASTM, pp. 315-328.
26. Hirschfeld, R. C. and Poulos, S. G. (1963) "High-Pressure Triaxial Tests on a Compacted Sand and an Undisturbed Silt," STP 361 - Laboratory Shear Testing of Soils, ASTM, 1963, pp. 329-339.
27. Insley, A. E. and Hillis, S. F. (1965) "Triaxial Shear Characteristics of a Compacted Glacial Till Under Unusually High Confining Pressures," Proceedings, 6th Int. Conf. on Soil Mechanics and Foundation Engineering, Vol. 1, Montreal, pp. 244-248.
28. Janbu, Nilmor (1963) "Soil Compressibility as Determined by Oedometer and Triaxial Tests," European Conference on Soil Mechanics and Foundation Engineering, Wissbaden, Germany, Vol. 1, pp. 19-25.
29. Kondner, R. L. (1963) "Hyperbolic Stress-Strain Response: Cohesive Soils," Journal of the Soil Mechanics and Foundations Division, ASCE, Vol. 89, No. SM1, February, 1963, p. 115.
30. Kondner, R. L. and Zelasko, J. S. (1963) "A Hyperbolic Stress-Strain Formulation of Sands," Proceedings of the 2nd PanAmerican Conference on Soil Mechanics and Foundation Engineering, Vol. 1, Brazil, 1963, p. 289.
31. Kulhawy, F. H. and Duncan, J. M. (1972) "Stresses and Movements in Oroville Dam," Journal of the Soil Mechanics and Foundations Division, ASCE, Vol. 98, No. SM7, Proc. Paper 9016, July 1972, pp. 653-665.
32. Kulhawy, F. H., Duncan, J. M. and Seed, H. B. (1969) "Finite Element Analysis of Stresses and Movements in Embankments During Construction," Report No. TE 69-4, Office of Research Services, University of California, Berkeley, California.
33. Lade, P. (1971) "The Stress-Strain and Strength Characteristics of Cohesionless Soils," Ph.D. Dissertation, University of California, Berkeley, California, August 1972.
34. Lee, K. L. (1965) "Triaxial Compressive Strength of Saturated Sand Under Seismic Loading Conditions," Dissertation presented to the University of California, Berkeley, in partial fulfillment of the requirements for the degree of Doctor of Philosophy.

35. Lefebvre, G., Duncan, J. M. and Wilson, E. L. (1973) "Three-Dimensional Finite Element Analyses of Dams," Journal of the Soil Mechanics and Foundations Division, ASCE, Vol. 99, No. SM7, Proc. Paper 9857, July, 1973, pp. 495-507.
36. Linell, K. A. and Shea, H. F. (1960) "Strength and Deformation Characteristics of Various Glacial Tills in New England," Research Conference on Shear Strength of Cohesive Soils, ASCE, Boulder, Colorado, pp. 275-314.
37. Marachi, N. (1969) "Strength and Deformation Characteristics of Rockfill Materials," Dissertation presented to the University of California, Berkeley, in partial fulfillment of the requirements for the degree of Doctor of Philosophy.
38. Marsal, R. J., Gomez, E. M., Nunez, A., Cuellar, R. and Ramos, R. M. (1965) "Research on the Behavior of Granular Materials and Rockfill Samples," Comision Federal de Electricidad, Mexico, D. F., February, 1965, 76p.
39. Marsal, R. J. (1967) "Large Scale Testing of Rockfill Materials," Journal of the Soil Mechanics and Foundations Division, ASCE, Vol. 93, No. SM2, March 1967, pp. 27-43.
40. Nobari, E. S. and Duncan, J. M. (1972) "Effect of Reservoir Filling on Stresses and Movements in Earth and Rockfill Dams," Report No. TE-72-1, University of California, Berkeley, January 1972.
41. Shannon and Wilson (1961) "Report on Soil Tests: Round Butte Dam Project," Shannon and Wilson, Soil Mechanics and Foundation Engineers, Seattle, Washington, July, 1961.
42. Shannon and Wilson (1963) "Report on Construction Control and Record Tests for Round Butte Dam," Shannon and Wilson, Soil Mechanics and Foundation Engineers, Seattle, Washington, 1963.
43. Shannon and Wilson (1964) "Report on Construction Control and Record Tests for Round Butte Dam," Shannon and Wilson, Soil Mechanics and Foundation Engineers, Seattle, Washington, 1964.
44. Sherman, W. C. and Trahan, C. C. (1968) "Analysis of Data from Instrumentation Program, Port Allen Lock," Technical Report S-68-7, U. S. Army Engineers, Waterways Experiment Station, Corps of Engineers, Vicksburg, Mississippi, September 1968.
45. Wong, Kai S. and Duncan, J. M. (1974) "Hyperbolic Stress-Strain Parameters for Nonlinear Finite Element Analyses of Stresses and Movements in Soil Masses," Report No. TE 74-3, University of California, Berkeley, July 1974.

APPENDIX - COMPUTER PROGRAM SP-5

This computer program evaluates the strength and stress-strain parameters  $c$ ,  $\phi$ ,  $\Delta\phi$ ,  $K$ ,  $n$ , and  $R_f$  using stress-strain data, and the bulk modulus parameters  $K_b$  and  $m$  using volume change data for conventional triaxial tests at various confining pressures. The program was developed by Kai Wong at the University of California, Berkeley in 1977.

The following data are required for the program:

Card 1 (10A8)

Columns 1-80 TITLEL. Title Card for program identification.

Card 2 (6I5,F10.0)

Columns 1-5 M.Number of stress-strain curves.  
 6-10 L.Number of volume-change curves.  
 11-15 JJ. If stress-strain data are given in terms of  $\sigma_1/\sigma_3$  vs  $\epsilon$ , JJ = 0. If stress-strain data are given in terms of  $(\sigma_1-\sigma_3)$  vs  $\epsilon$ , JJ = 1.  
 16-20 IPUNCH. If no punched output is desired, IPUNCH = 0. If punched output is desired, IPUNCH = 1.  
 21-25 ICHECK. If ICHECK = 1, corresponding values of  $(\sigma_1-\sigma_3)$  and  $\epsilon$  will be calculated using the parameters determined and the values printed. These are useful in checking the correspondence of the data and the parameters. If ICHECK = 0, these values are not calculated or printed.  
 26-30 ICOND. For ICOND = 0, a straight-line failure envelope is fitted to the data, and values of  $c$  and  $\phi$  are determined. For ICOND = 1, a curved envelope is fitted to the data, and values of  $\phi_0$  and  $\Delta\phi$  are determined. (See equation 14 and Figs. 13 and 14.)

31-40 Atmospheric pressure, expressed in the system of units used in the tests.

$$\begin{array}{ll}
 p_a = 14.7 \text{ lb/in}^2 & p_a = 1.033 \text{ kg/cm}^2 \\
 p_a = 2116 \text{ lb/ft}^2 & p_a = 10.33 \text{ metric ton/m}^2 \\
 p_a = 2.116 \text{ k/ft}^2 & p_a = 101.4 \text{ kN/m}^2 \\
 p_a = 1.058 \text{ t/ft}^2 &
 \end{array}$$

Card(s) 3 (6F10.0)

Columns 1-10 Confining pressure,  $\sigma_3$ .

- 11-20 Stress ratio at failure,  $(\sigma_1/\sigma_3)_f$  or stress difference at failure,  $(\sigma_1 - \sigma_3)_f$ .
- 21-30 Axial strain at 70% stress level (percent).
- 31-40 Axial strain at 95% stress level (percent).
- 41-50 Volumetric strain at 70% stress level (percent).

The input volumetric strain at 70% must be compressive and be less than or equal to the maximum compressive volumetric strain.

Repeat, one card for each test, total of M cards.

```

PROGRAM SPS (INPUT,OUTPUT,PUNCH,TAPE1=INPUT)
COMMON M,L,KK,JJ,XIN(20),YIN(20),XSLOPE,YINTER,
1P(20),DPA(20),DPB(20),DPF(20),PA,
2EAA(20),EAB(20),EVA(20),EVB(20),ERA(20),ERB(20),
3COHESN,ANGL1,DANGL1,
4XK,XN,RAVE,XKB,XM,
5TITLE1(10),
6EI(20),PPA(20),B(20)

```

#### INPUT INFORMATION OF EACH SOIL

```

1 READ 100, TITLE1
  IF (EOF(1)) 2,3,2
2 STOP
3 CONTINUE
  READ 120,M,L,JJ,IPUNCH,ICHECK,ICOND,PA
  MM = M
  PRINT 130
  PRINT 200,TITLE1
  PRINT 190

```

#### EVALUATION OF EI AND RF

```

KB=0
XM=0.0
XKB=0.0
XMAX = 0.0
XMIN = 1000.0
PR=0.0
PRINT 140
DO 5 I=1,M
  READ 150,P(I),DPF(I),EAA(I),EAB(I),EVA(I)
  IF(JJ.EQ.1) GO TO 4
  DFF = DPF(I)
  DPF(I)=DPF(I)*P(I)-P(I)
4  DPA(I) = 0.7*DPF(I)
  DPB(I) =0.95*DPF(I)
  EAA(I)=0.01*EAA(I)
  EAB(I)=0.01*EAB(I)
  TA=EAA(I)/(DPA(I))
  TB=EAB(I)/DPB(I)
  SLOPE=(TB-TA)/(EAB(I)-EAA(I))
  EI(I)=2.0/(TB+TA-SLOPE)*(EAB(I)+EAA(I)))
  RF =DPF(I) *SLOPE
  AAA = 100.0*EAA(I)
  AAB = 100.0*EAB(I)
  PRINT 160, P(I),DPF(I),AAA,AAB,EVA(I)
  SIGMA3 = P(I)
  IF(SIGMA3.LT.XMIN) XMIN = SIGMA3
  IF(SIGMA3.GT.XMAX) XMAX = SIGMA3
  PR = PR + RF
5 CONTINUE
  RAVE=PR/M
  PRINT 170,M,L,JJ,IPUNCH,ICHECK,ICOND,PA

```

#### STRESS RANGE

```

XMIN = XMIN/PA*1.058

```

XMAX = XMAX/PA\*1.058

EVALUATION OF K AND N

```
DO 6 I=1,M
PPA(I)=P(I)/PA
EI(I)=EI(I)/PA
XIN(I)= ALOG10(PPA(I))
6 YIN(I)= ALOG10(EI(I))
KK = 0
CALL LESQRE
XN=XSLOPE
XK=YINTER
K=XK
```

EVALUATION OF COHESION AND FRICTION ANGLE

```
IF(ICOND.EQ.0) GO TO 7
CALL ANGLL
PRINT 180
GO TO 15
7 DO 8 I=1,M
XIN(I) = (DPF(I) + 2*P(I))/2.0
8 YIN(I) = DPF(I)/2.0
KK=1
CALL LESQRE
YI = YINTER
ANGLE = XSLOPE
SOLD = 1000.0
IF (XSLOPE.GE.0.0) GO TO 10
ANGLE = 0.0
SUM = 0.0
DO 9 J = 1,M
9 SUM = SUM + YIN(J)
YI = SUM/M
10 IF (YINTER.GE.0.0) GO TO 14
YI = 0.0
SOLD=100.0
R = 0.04
DO 12 I = 1,10
XSLOPE = XSLOPE - R
SUM = 0.0
DO 11 J=1,M
11 SUM = SUM + (YIN(J) - XSLOPE*XIN(J))**2
IF(SUM.GT.SOLD) R = (-0.5)*R
IF(SUM.LE.SOLD) SOLD = SUM
IF(ABS(R).LE.0.025) GO TO 13
12 CONTINUE
13 XSLOPE = SOLD
14 CONTINUE
ANGL1 = ASIN(ANGLE )/3.1416*180.0
COHESN = YI / COS(ANGLE)
COHESN = COHESN/PA*1.058
DANGLE1 = 0.0
15 CONTINUE
IF(L.EQ.0)GO TO 25
```

EVALUATION OF KB AND M

```

DO 21 I=1,L
B(I)=70.0*DPF(I)/3.0/EVA(I)/PA
XIN(I)=ALOG10(PPA(I))
21 YIN(I)=ALOG10(B(I))
KK=0
CALL LESQRE
XM=Xslope
XKB=YINTER
IF(XM.GE.0.0)GO TO 23
XM=0.0
SUM=0.0
DO 22 I=1,L
22 SUM=SUM+B(I)
XKB=SUM/L
23 KB=XKB
25 CONTINUE

PRINT 190
PRINT 270
IF (ICOND.NE.0) GO TO 16
PRINT 280,XMIN,XMAX,M,COHESN, ANGL1, K, XN, RAVE,KB,XM
PRINT 190
GO TO 17
16 PRINT 290,XMIN,XMAX,M,COHESN, ANGL1,DANGL1, K, XN, RAVE,KB,XM
PRINT 190
17 CONTINUE
PRINT 330
PRINT 340,(PPA(I),EI(I),B(I),I=1,M)
PRINT 190

IF(IPUNCH.EQ.0)GO TO 19
PUNCH 110, TITLE1
IF (ICOND.NE.0) GO TO 18
PUNCH 310,XMIN,XMAX,M,COHESN, ANGL1, K, XN, RAVE
GO TO 19
18 CONTINUE
PUNCH 320,XMIN,XMAX,M,COHESN, ANGL1,DANGL1, K,XN,RAVE
IF(L.GT.0)PUNCH 370,XKB,XM
19 IF(ICHECK.EQ.0)GO TO 1
CALL CHECK1
GO TO 1
100 FORMAT(10A8)
110 FORMAT (10A8)
120 FORMAT(6I5,F10.0)
130 FORMAT ('1','*INPUT*',1*XXXXXXXXXXXXXX)
140 FORMAT('0',4X,'SIGMA3',3X,'(S1-S3)',10X,'EPS1',12X,'EPS1', 11X,
1'EPSV',10X,'EPSV', /12X,'AT FAILURE',5X,'70 PERCENT', 6X,'95 PERCE
2NT', 5X,'70 PERCENT')
150 FORMAT (6F10.0)
160 FORMAT (' ',2F10.2,4F15.4)
170 FORMAT('0','M=',I3,4X,'L=',I3,4X,'JJ=', I2,4X,'IPUNCH=',I2,4X,
1'ICHECK=',I2,4X,'ICOND=',I2,4X,'PA=',F10.5)
180 FORMAT('0','* COHESIONLESS SOIL ',1*XXXXXXXXXXXXXX)
190 FORMAT ('0','* ',1*XXXXXXXXXXXXXX)
200 FORMAT ('0',10A8/)
270 FORMAT('0',2X,'STRESS RANGE',3X,'NUMBER',4X,'C',4X,'FRICTION',5X,

```

```

1K',6X,'N',4X,'RF',5X,'KB',5X,'M'/6X,'(TSF)',6X,'OF TEST',2X,'(TSF)
2',3X,'ANGLE')
280 FORMAT('0',F5.1,'-',F5.1,6X,I2,4X,F5.2,F6.1,7X,I7,F6.2,F6.2,I7,F6.
12)
290 FORMAT('0',F5.1,'-',F5.1,6X,I2,4X,F5.2,F6.1,1X,'(',F4.1,')',I7,F6.
12,F6.2,17,F6.2)
310 FORMAT( F5.1,' -',F5.1,7X,I2,3X,F10.2,F9.1,13X,I5, 2F9.2/1X)
320 FORMAT( F5.1,' -',F5.1,7X,I2,3X,F10.2,F9.1,' (',F5.2,')', 5
1X,I5, 2F9.2/1X)
330 FORMAT('0',5X'S3/PA',5X,'EI/PA',6X,'BPA')
340 FORMAT(' ',3F10.3)
370 FORMAT(F10.2,F10.4)
END
SUBROUTINE LESQRE
COMMON M,L,KK,JJ,XIN(20),YIN(20),XSLOPE,YINTER
X=0.0
Y=0.0
XX=0.0
XY=0.0
DO 10 I=1,M
X=X+XIN(I)
Y=Y+YIN(I)
XX= XX+XIN(I)*XIN(I)
10 XY=XIN(I)*YIN(I)+XY
XSLOPE = (M*XY-XXY)/(M*XX-XXX)
YZ = (Y*XX-XX*Y)/(M*XX-XXX)
IF (KK.EQ.0) GO TO 20
YINTER = YZ
GO TO 30
20 YINTER = 10.0*YZ
30 RETURN
END
SUBROUTINE ANGLL
COMMON M,L,KK,JJ,XIN(20),YIN(20),XSLOPE,YINTER,
1P(20),DPA(20),DPB(20),DPF(20),PA,
2EAA(20),EAB(20),EVA(20),EVB(20),ERA(20),ERB(20),
3COHESN,ANGL1,DANGL1
DO 100 I=1,M
AANG = (DPF(I)/2.0)/((DPF(I) +2*P(I))/2.0)
ANG = ASIN(AANG)/3.1416*180.0
XIN(I)= ALOG10(P(I)/PA)
YIN(I)= ANG
100 CONTINUE
COHESN=0.0
KK=1
CALL LESQRE
ANGL1 = YINTER
DANGL1 = XSLOPE*(-1.0)
RETURN
END
SUBROUTINE CHECK1
COMMON M,L,KK,JJ,XIN(20),YIN(20),XSLOPE,YINTER,
1P(20),DPA(20),DPB(20),DPF(20),PA,
2EAA(20),EAB(20),EVA(20),EVB(20),ERA(20),ERB(20),
3COHESN,ANGL1,DANGL1,
4XX,XN,RAVE,XKB,XM,
5TITLE1(10),
6EI(20),PPA(20),B(20)
X = COHESN/1.058*PA
ANGL2 = ANGL1
DANGL2=DANGL1
DO 1000 I = 1,M
ANGL1= (ANGL2-DANGL1*ALOG10(P(I)/PA))/57.29578

```

```

DDF = (2.0*X*COS(ANGL1) + 2.0*P(I)*SIN(ANGL1))/(1.0 - SIN(ANGL1))
DFF=DDF
IF(JJ.EQ.0) DDF=(DDF+P(I))/P(I)
E=XK*PA*(P(I)/PA)**XN
Z=XKB*PA*(P(I)/PA)**XM
ANGGG=ANGL1/3.1416*180.0
PRINT 100,TITLE1
100 FORMAT('1',10A8)
PRINT 200,P(I),PA,DDF,COHESN,ANGGG, XK,XN,RAVE,XKB,XM
IF(JJ.EQ.1) GO TO 115
PRINT 210
GO TO 120
115 PRINT 220
120 CONTINUE
C
ESP1 = 0.0
DO 145 J = 1.45
C
C      HYPERBOLIC FITTING OF STRESS-STRAIN CURVE
C
IF(J.LE.20)      ESP1= ESP1 + 0.0025
IF(J.GT.20)      ESP1= ESP1 + 0.01
C
C
SIG13 = ESP1 /(1.0/E + ESP1*RAVE/DFF)
SGG13 = SIG13
IF(JJ.EQ.1) GO TO 125
SIG13=(SIG13+P(I))/P(I)
125 IF(L.GT.1) GO TO 130
ESPP=ESP1*100.0
PRINT 230,ESPP,SIG13
IF(SIG13.GT.DDF) GO TO 1000
GO TO 145
130 ESPVA=SGG13*100.0/3.0/Z
ESPP=ESP1*100.0
C
C
140 PRINT 240, ESPP, SIG13, ESPVA
IF(SIG13.GT.DDF) GO TO 1000
145 CONTINUE
150 CONTINUE
200 FORMAT('0','SIG3 ****',F10.4,10X,'ATMOSHPERIC PRESSUR
1E =',F10.4/1H,
1      'STRESS AT FAILURE ***',F10.4/ 1H0,
4      'COHESION (TSF) ****',F10.4/ 1H ,
5      'ANGLE ****',F10.4/ 1H0,
2      'K ****',F10.4/ 1H ,
3      'N ****',F10.4/ 1H ,
6      'RF ****',F10.4/ 1H0,
8      'KB****',F10.4/ 1H ,
7      'M ****',F10.4/ )
210 FORMAT('0',10X,'PARAMETERS KB,M'
16X, 'ESP1 SIG1/SIG3   ESPV'|)
220 FORMAT('0', 10X, 'PARAMETERS KB,M'
16X, 'ESP1 SIG1-SIG3   ESPV'|)
230 FORMAT (' ',2F10.2)
240 FORMAT (' ',2F10.2,F10.3)
RETURN
END

```